齒醫科學博士學位論文

# Trapidil promotes osteogenesis by activating the signaling of BMP

뼈형성단백질 신호전달경로 활성화를 통한

트라피딜의 골형성 촉진

2018년 2월

서울대학교 대학원

치의생명과학과 세포및발생생물학 전공

김 봉 준

# Trapidil promotes osteogenesis by activating the signaling of BMP

by

**Bongjun Kim**

Advisor:

**Prof. Zang Hee Lee DDS, Ph.D**

A Thesis Submitted in Partial Fulfillment of the
Requirements for the Degree of Doctor of Philosophy

**February, 2018**

**Division of Cell and Developmental Biology**
**Department of Dental Science, School of Dentistry**
**Seoul National University**

# BMP2 신호전달 활성화를 통한 트라피딜의 골형성 촉진

지도교수 이장희

이 논문을 치의과학박사학위논문으로 제출함

2017 년 12 월

서울대학교 대학원

치의생명과학과 세포및발생생물학 전공

김 봉 준

김봉준의 박사학위논문으로 인준함

2017 년 12 월

위 원 장 민 병 무 (인)

부위원장 이 장 희 (인)

위 원 김 현 만 (인)

위 원 김 홍 희 (인)

위 원 이 수 영 (인)

# Trapidil promotes osteogenesis by activating the signaling of BMP

by

**Bongjun Kim**

Advisor:

**Prof. Zang Hee Lee DDS, Ph.D**

A Thesis Submitted in Partial Fulfillment of the
Requirements for the Degree of Doctor of Philosophy

**December, 2017**

**Doctoral Committee:**

Professor Byung-Moo Min, Chairman

Professor ZANG HEE LEE, Vice chairman

Professor HYUN-MAN KIM

Professor Hong-Hee Kim

Professor Soo Young Lee

# ABSTRACT

## Trapidil promotes osteogenesis by activating the signaling of BMP

Bongjun Kim

Department of Cell and Developmental Biology

School of Dentistry, Seoul National University

(Advised by Prof. Zang Hee Lee, DDS, Ph. D.)

Bone is a continuously renewing tissue which its mass is finely balanced by the bone-forming and -resorbing cells, osteoblasts and osteoclasts, respectively; however, an imbalance between these processes causes osteopathic diseases, such as osteoporosis. For osteoporosis therapy, anti-osteoclastic drugs are used to attenuate the upregulated osteoclast activity. However, anti-osteoclasts agents cannot restore already destroyed bone. Thus, bone anabolic agents are required. Studies have shown that inhibition of platelet-derived growth factor

receptor (PDGFR) signaling promotes osteogenesis *in vitro*. However, the therapeutic efficacy of inhibiting PDGF signaling in bone regeneration *in vivo* and the specific mechanisms by which PDGFR signaling inhibits osteogenic differentiation remain unclear. In the present study, the osteogenic effect of PDGFR inhibition was examined using a PDGFR antagonist, trapidil, *in vivo* and *in vitro*, and its mechanisms were evaluated. A rat calvarial defect model was analyzed using micro-computed tomography and histology to determine the pro-osteogenic effect of trapidil *in vivo*. Trapidil greatly promoted bone regeneration of a defected rat calvariae. In addition, primary mouse calvarial osteoblast precursors were cultured in osteogenic differentiation medium containing trapidil to study the mechanisms. Trapidil induced phosphorylation of Smad1/5/9 and mitogen-activated protein kinase (MAPK), enhancing the expression of runt-related transcription factor 2 (Runx2), a crucial transcription factor for osteogenesis. The pro-osteogenic effects of trapidil were inhibited by LDN193189, a specific inhibitor of the bone morphogenetic protein receptor (BMPR), activin receptor-like kinase 2 (ALK2) and ALK3, and by treatment with a BMP

antagonist noggin, as well as ALK3 depletion. Moreover, trapidil showed a synergistic effect with human recombinant BMP2 on osteogenic differentiation. In conclusion, our results demonstrate that trapidil induces osteogenesis through activation of BMP signalling, and that the attenuated PDGFR signalling is involved in the bio-reactivity of a type Ⅰ BMP receptor, ALK3.

---

**Keywords**: Trapidil, Osteoblast, PDGF, BMP, Osteogenesis

**Student Number**: 2013-23553

# CONTENTS

# LIST OF FIGURES

# LIST OF TABLES



# ABBREVIATIONS

| | |
|---|---|
| **ALP** | alkaline phosphatase |
| **BMP** | bone morphogenetic protein |
| **BMPR** | bone morphogenetic protein receptor |
| **BMSC** | bone marrow stromal cell |
| **H&E** | hematoxylin and eosin |
| **KD** | kinase dead |
| **MAPK** | mitogen-acitvated protein kinase |
| **MSC** | mesenchymal stem cell |
| **pNPP** | nitrophenyl phosphate |
| **PDGF** | platelet-derived growth factor |
| **PDGFR** | platelet-derived growth factor receptor |
| **shRNA** | short hairpin RNA |
| **WT** | wild type |

# Introduction

Bone is a continuously renewing tissue that is exquisitely balanced by bone-forming and -resorbing cells, the osteoblasts and osteoclasts, respectively (Figure 1). However, an imbalance between osteoclastic bone resorption and osteoblastic bone formation causes osteopathic diseases such as osteoporosis (*1*, *2*). Osteoporosis is a common age-related bone-degenerative disease that often occurs in postmenopausal women because of increased osteoclast activity as a result of estrogen deficiency (*3*). Current osteoporosis therapies are primarily targeted at reducing bone resorption; however, these agents secondarily reduce bone formation and cause rare and potentially serious side effects such as osteonecrosis of the jaw (*2*, *4*). In addition, anti-resorptive agents for osteoporosis have limitations for restoring already impaired bones. Therefore, advanced osteogenic drugs are needed to treat osteoporosis. Parathyroid hormone preparations are currently the only drugs approved by the US Food and Drug Administration (FDA) that stimulate bone formation. However, these drugs also enhance bone resorption, and their anabolic effect wanes over time. Furthermore, their use is limited to 2 years because of potential osteosarcoma

development (*2, 4, 5*). Thus, new bone anabolic agents that are safe and efficient for long-term use are urgently needed.

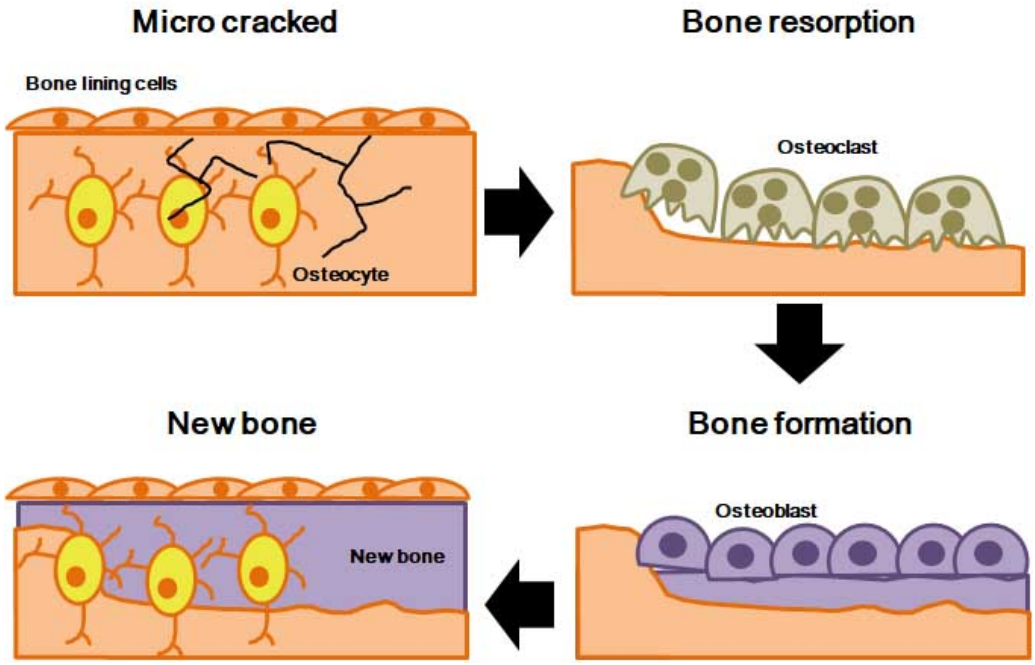


**Figure 1. Physiological bone remodeling**

Bone remodeling follows coordination of distinct and sequential phases of the process. The remodeling cycle is composed of six sequential phases, namely, quiescence, activation, resorption, reversal, formation, and termination. Activation precedes resorption, which precedes reversal, with mineralization as the last step. The first stage of bone remodeling involves detection of an initiating remodeling signal, which has usually been described as resorption by osteoclasts. In the resorption phase, osteoblasts respond to signals generated by osteocytes or direct endocrine activation signals, recruiting osteoclast

precursors to the remodeling site. The resorption phase is of limited duration depending on level of the stimuli responsible for osteoclast differentiation and activity. It is followed by the reversal phase that is characterized by disappearance of almost all osteoclasts. The formation phase is distinct by complete replacement of osteoclastic cells with osteoblastic cells. The termination signals of bone remodeling include the terminal differentiation of the osteoblast. The resting bone surface environment is maintained until the next wave of remodeling is initiated.

Osteogenesis is under the control of multiple factors including bone morphogenetic proteins (BMPs) and platelet-derived growth factors (PDGFs) (*6*). As the name implies, BMPs were originally discovered by their ability to induce new bone formation (*7*). Four type I (activin receptor-like kinase [ALK] 1, 2, 3, and 6) and three type II (BMP receptor type IIB [BMPRIIB], activin type IIA [ACTRIIA], and ACTRIIB) BMP receptors with serine/threonine kinase activity are involved in the BMP signaling pathway (*8*) (Figure 2). The ligand-bound type II receptor activates type I receptor kinase through phosphorylation of the glycine-serine domain, which in turn directly phosphorylates Smads (including Smad1, Smad5, and Smad9) or activates mitogen-activated protein kinase (MAPK) pathways including extracellular signal-regulated kinase (ERK), c-Jun N-terminal kinase (JNK), and p38. Phosphorylated Smad1/5/9 form heteromeric complexes with Smad4 and translocate into the nucleus to regulate the transcription of various target genes including the inhibitor of DNA binding 1, HLH protein (*Id-1*), resulting in the promotion of osteogenesis (*9-12*). In addition, the activity or expression of runt-related transcription factor 2 (Runx2), a crucial transcription factor for osteogenic differentiation, is positively regulated by BMPR-activated signal pathways such as ERK, JNK, p38, and Smads (*13, 14*). Upregulated/activated Runx2, in turn, promotes the expression of multiple osteogenic genes including

tissue-nonspecific alkaline phosphatase (*TNAP*), collagen type 1 alpha 1 (*Col1a1*), osterix (*Osx)*, osteocalcin (bone γ-carboxyglutamate protein [*Bgalp2*]*)*, and bone sialoprotein (*BSP*) (*15*).

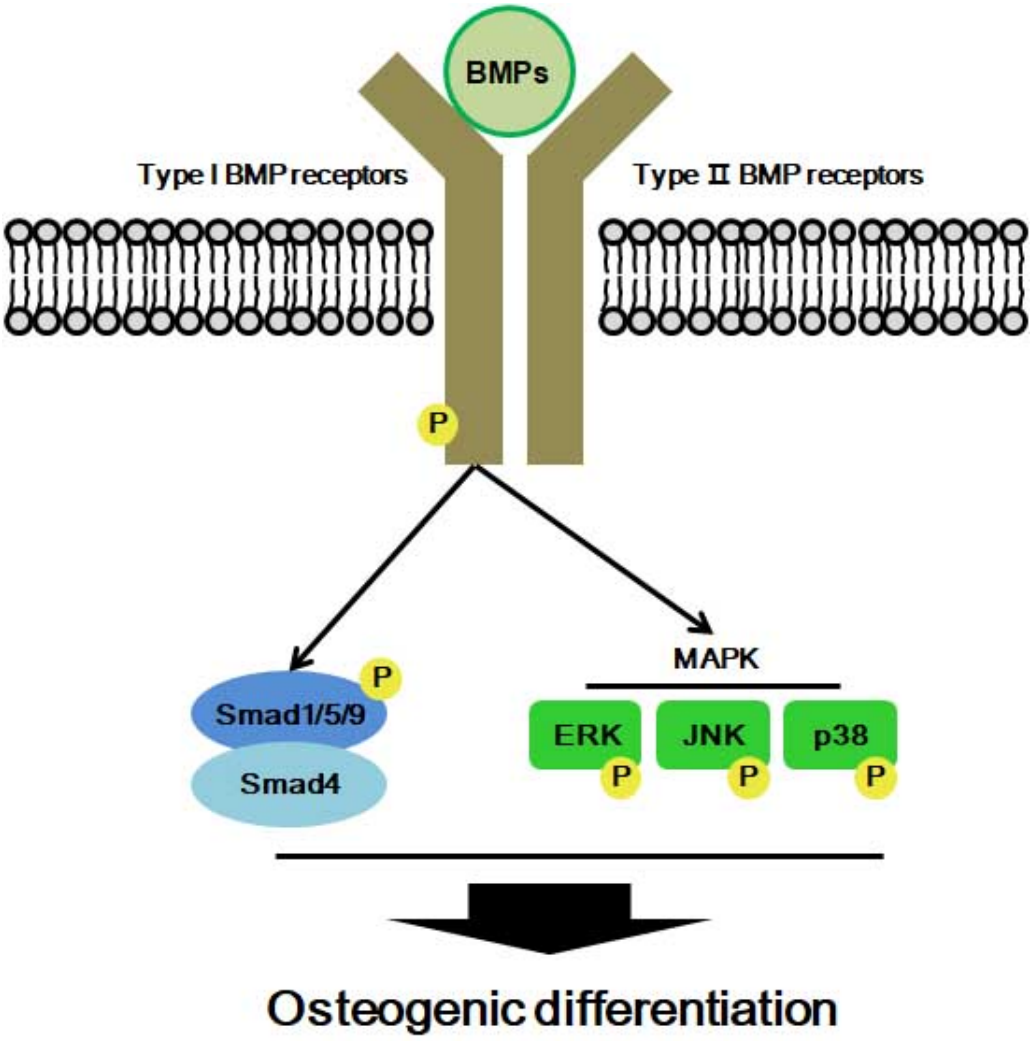


**Figure 2. Schematic overview of the BMP signaling pathway**

BMPs interaction with surface receptors induces heteromeric complex formation between specific type II and type I receptors. This activity is regulated by extracellular regulators and type III receptors/co-receptors. After

being activated by type II receptors, the type I receptors phosphorylate Smad1/5/9 (R-Smads) to propagate the signal into the cell. Smad1/5/9 form heteromeric complexes with Smad4 (Co-Smad) and translocate to the nucleus where, by interacting with other transcription factors, they regulate target gene expression (canonical Smad signaling pathway). Activated MAPKs can regulate R-Smad activation by a direct phosphorylation or through their downstream effectors molecules. Activated MAPKs can translocate to the nucleus to phosphorylate a number of transcription factors (TF), such as serum response factor (SRF), ternary complex factor (TCF) family members, activator protein 1 (AP1) complexes and activating transcription factor 2 (ATF2), thereby changing target gene transcription.

PDGFs are composed of five ligand dimers, PDGF-AA, -BB, -AB, -CC, and -DD, which bind to three receptor dimmers, PDGF receptor (PDGFR) αα, αβ, and ββ, with different affinities. The PDGFs transduce overlapping but not identical cellular signals such as Src, JNK, Akt, and phospholipase C γ (PLCγ), to regulate cellular properties including proliferation and migration (*16-19*) (Figure 3). Osteoblasts and their precursor cells, mesenchymal stem cells (MSCs), have been reported to express both PDGFR and its ligands, by which PDGF signaling positively regulates proliferation and chemotaxis (*20-24*). On the other hand, PDGF signaling has been shown to negatively regulate osteogenesis. Depletion of PDGFRβ on mouse MSCs promotes osteogenic differentiation (*25*). PDGF-BB inhibits osteogenic differentiation of MC3T3-E1 cells, an osteoblastic cell line (*25, 26*), and inhibition of PDGFRs with imatinib or AG-1295 promotes differentiation of mouse calvarial osteoblasts and MC3T3-E1 cells, respectively (*27, 28*). However, the specific mechanisms by which PDGFR signaling inhibits osteogenesis remain to be clarified.

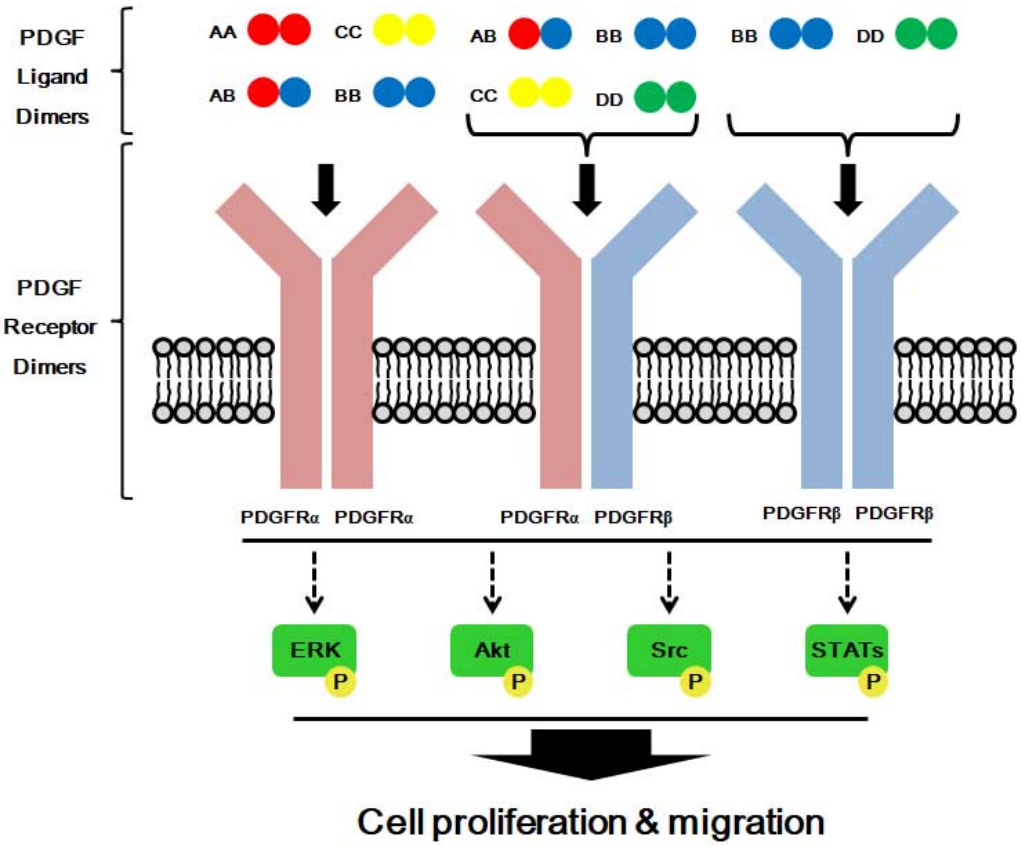


**Figure 3. Binding of the five PDGF isoforms induces different homo- and heterodimeric complexes of PDGFRα and PDGFRβ**

The PDGF isoforms are synthesized as precursor molecules with signal sequences, precursor sequences and growth factor domains. After dimerization, the isoforms are proteolytically processed to their active forms which bind to the receptors. Five different kinds of PDGF dimmers (PDGF-AA, PDGF-AB, PDGF-BB, PDGF-CC, and PDGF-DD) bind to receptor alpha (α) or receptor

beta (β) with distinct affinities, respectively. Ligand-induced dimerization induces autophosphorylation of the receptors, which activates their kinases and create docking sites for SH2-domain-containing signaling molecules, some of which are indicated in the figure. Activation of these signaling pathways promotes cell growth, survival, migration and actin reorganization.

Trapidil, a vasodilator and an anti-platelet agent, antagonizes PDGFRs as a competitive inhibitor and regulates the expression of PDGFRs (*29-32*). Trapidil has also been reported to inhibit several molecules, including phosphodiesterase, thromboxane A2, and CD40 signaling, and to activate protein kinase A (*33-36*). Accumulating evidence shows that trapidil is clinically effective in coronary artery disease (*37*), and it has been shown to be effective in the treatment of parathyroid bone diseases by suppressing the development of osteitis fibrosa in an animal model of chronic hyperparathyroidism (*38*, *39*). In particular, previous study has shown an anti-osteoclastogenic effect of trapidil (*40*). However, the effects of trapidil on osteogenesis remain unknown.

In this study, the hypothesis that trapidil promotes osteogenesis by regulating PDGF signaling was examined. To investigate the effect of PDGFR inhibition with trapidil on osteogenesis, both *in vivo* and *in vitro* experiments were performed. First, a rat calvarial defect model was used to assess the anabolic potential of trapidil. Second, the *in vitro* osteogenic potency of this agent was analyzed using various osteoblastic cells such as primary mouse calvarial osteoblast precursors, primary mouse bone marrow stromal cells (BMSCs), mouse osteoblast cell line MC3T3-E1 cells, and mouse myoblast cell

line C2C12 cells. The results of the present study showed that trapidil enhanced osteogenesis both *in vivo* and in *vitro*. In addition, the molecular mechanisms underlying the pro-osteogenic effect of trapidil were elucidated.

# Materials and methods

## Animals

Animal studies are reported in compliance with the ARRIVE guidelines (*41*, *42*). All animal procedures were reviewed and approved by the animal care committee of the Institute of Laboratory Animal Resources of Seoul National University (approval protocol number SNU-130416-1).

## Rat calvarial defect model

For critical-size calvarial defects, male Sprague-Dawley rats were used (average weight 280 g and 2 month-old). Rats were purchased from the Jackson Laboratory (Bar Harbor, ME). Trapidil (Sigma, St Louis, MO, USA) was dissolved in distilled water. Absorbable collagen sponges (BiolandKorea, Cheonan, Korea) were loaded with recombinant human BMP 2 (2 mg per scaffold, 15-mL volume; rhBMP2; Pepro-Tech, Rocky Hill, NJ, USA), Trapidil (4 mg per scaffold, 15-mL volume), or PBS (15-ml volume) (n = 6 per group) as previously described ((*43-45*). The animals were randomly assigned to the different treatment groups. The surgical procedures for the creation of an 8-mm

circular defect in the calvaria and implantation of the collagen sponge were carried out as described previously (*45*). The rats were euthanized at 3 weeks after surgery, and whole calvaria were fixed in 4% paraformaldehyde for 24 hours at 4 ℃ and then analyzed by μCT scanning. Details for the μCT scans are illustrated below.

## μCT and histomorphometric analysis

μCT was performed with the SMX-90CT system (90 kVp, 109 mA,and 180-ms integration time; Shimadzu, Kyoto, Japan). Scans then were integrated into 3D voxel images (1024 X 1024 pixel matrices). All bone images were reconstructed by using the VG Studio MAX 1.2.1 program (Volume Graphics, Heidelberg, Germany) by use of standard procedures. The regenerated bone volume/tissue volume (BV/TV, %) was calculated and expressed with TRI/3D-VIE (RATOC System Engineering, Kyoto, Japan) according to standard formulas and nomenclature. Calvarial thickness (mm) was calculated with OsteoMeasure XP Version 1.01 (OsteoMetrics, Decatur, GA, USA) according to standardized protocols.

The specimens were then decalcified with 12% EDTA for 4 weeks and embedded in paraffin. Paraffin-embedded samples were sectioned at a thickness of 6 μm and stained with H&E (Sigma, St Louis, MO, USA) and

Masson's trichrome (Millipore, Billerica, MA, USA) according to the manufacturer's instruction.

## Cell culture and osteogenic differentiation

Primary osteoblast precursors were isolated from calvariae of newborn mice as described previously (*45*). Primary mouse bone marrow derived stromal cells (mBMSCs) were isolated from femora and tibiae of mice according to the protocol described by (*46*). MC3T3-E1 cells and C2C12 cells were obtained from the American Type Culture Collection (Manassas, VA, USA) and used between four and ten passages. Osteoblast precursors and MC3T3-E1 cells were cultured in a minimum essential medium (a-MEM) complete medium (a-MEM containing 10% FBS, 50 units/mL of penicillin and 50 mg/mL of streptomycin). mBMSCs were cultured in a DMEM containing 15% FBS, 50 units/mL of penicillin, and 50mg/mL of streptomycin. C2C12 cells were cultured in DMEM containing 15% FBS, 50 units/mL of penicillin, and 50mg/mL of streptomycin. Osteoblast precursors were differentiated with or without trapidil, LDN193189 (Sigma, St Louis, MO, USA), recombinant mouse noggin (Pepro-Tech, Rocky Hill, NJ, USA), imatinib (Sigma, St Louis, MO, USA), PDGFRi IV (Millipore, Bedford, MA), or PDGFRi V (Millipore, Bedford, MA). To induce differentiation, 5 X $10^4$ osteoblast precursors or

mBMSCs, or 2 X $10^4$ MC3T3-E1 cells or C2C12 cells were seeded on 48-well plates pre-coated with collagen (for osteoblast precursors and mBMSCs) or on uncoated plates (for MC3T3-E1 cells and C2C12 cells) and then further cultured in osteogenic medium : for osteoblast precursors a-MEM complete medium containing 10mM β-glycerophosphate (Sigma, St Louis, MO, USA) and 50 mg/mL of ascorbate-2-phosphate (Sigma, St Louis, MO, USA)), and for MC3T3-E1 cells a-MEM complete medium containing 10mM β-glycerophosphate and 50 mg/mL of ascorbate-2-phosphate, and for mBMSCs a-MEM complete medium containing 10mM β-glycerophosphate, 50 mg/mL of ascorbate-2-phosphate and 0.1μM of dexamethasone (Sigma, St Louis, MO, USA), and for C2C12 DMEM complete-medium were used. Cells with recombinant human BMP2 (rhBMP2; Pepro-Tech, Rocky Hill, NJ, USA) were used as positive control. The osteogenic medium was replaced every 3 days. An ALP liquid assay activity assay and an ALP stain were performed 3 days after the induction of differentiation. The cultures also were stained for extracellular matrix calcification by 0.2% alizarin red S (pH 4.3; Sigma, St Louis, MO, USA) on day 14.

## ALP staining and activity

Quantitative analysis of ALP activity was performed by using the p-

Nitrophenyl Phosphate (pNPP) Liquid Substrate System (Sigma, St Louis, MO, USA) according to the manufacturer's instructions. In brief, ALP activity in cell lysates was determined with pNPP as the substrate in an assay buffer containing 5mM $MgCl_2$ and 50mM $Na_2CO_3$. Absorbance at 405nm was measured by using a microplate reader, and ALP activity was calculated from a standard curve. For ALP staining, cells were fixed with 10% formalin, incubated with 0.1% Triton X-100 for 5 minutes, and then stained by using the Leukocyte Alkaline Phosphatase Kit (Sigma, St Louis, MO, USA) following the manufacturer's procedure.

## Electroporation and luciferase reporter assay

For the Id1 (inhibitor of DNA binding/differentiation 1) reporter gene assay, pGL3-1d1-Luc reporter plasmid (Addgene, Cambridge, MA, USA) or pGL3 empty vector were electroporated into primary osteoblast precursors using the Neon Transfection System (Invitrogen) according to the manufacturer's instructions. At 24 hours after electroporation, cells were treated with trapidil or rhBMP2 for 24 hours. Luciferase activity was quantified by using an enhanced luciferase assay kit (BD Biosciences, Franklin Lakes, NJ, USA).

For overexpression of Akt constructs, pMSCV, pMSCV-WT Akt (wild-type Akt), pMSCV-KD Akt (kinase dead Akt, dominant negative mutant of Akt) (Addgene) construcs were used. Cells were electroprated with Akt constructs described above and after 24 hours of electroporation, cells were used for osteogenic differentiation and western blot analysis.

## Viral gene transduction

Retroviral transduction was performed as described previously (*47*). pMX-puro, pMX-puro-WT CREB (wild-type CREB), pMX-puro-S133A CREB (phosphorylation defective mutant of CREB at serine 133), and pMX-puro-K CREB (DNA binding domain mutant of CREB) construcs were used for retroviral transduction (*47*). In brief, retrovirus packaging was performed by transient co-transfection of these pMX vectors with VSV-G and PEQ-PAM into Plat-E retroviral packaging cells. After incubation in fresh medium for 2 days, culture supernatants of the retrovirus-producing cells were collected, and added to cells with 5 lg/ml polybrene (Sigma, St. Louis, MO) for 8 h. Infected cells were cultured for 1 day and were then further cultured with puromycin (2 lg/ml) for 2 days to remove uninfected cells. Lentiviral vector was prepared according to the manufacturer's instructions (Sigma–Aldrich, St. Louis, MO, USA). In

brief, 293FT cells were plated at $1 \times 10^6$ cells/well into 6-well plate and incubated overnight. The next day, the cells were transfected with 1.2μg of shRNA transfer vector, 0.3μg of pMD2G vector and 0.9μg of psPAX2 vector with lipofectamine LTX reagent (Invitrogen). Virus-containing cell culture supernatant was collected twice at 48 and 72 h after transfection, and was filtered with a 0.45-μm pore-size filter (Millipore, Bedford, MA). Viral particle-associated p24 antigen was quantitated by use of an HIV p24 ELISA kit (Cell Biolabs, San Diego, CA) and converted to functional viral titer. Lentiviral vectors were aliquoted and stored in a −80°C freezer until used. Two kinds of shALK2 (TRCN00000321758 or TRCN0000321754) or two kinds or shALK3 (TRCN0000274550 or TRCN0000274499) were used. Luciferase shRNA was used as a control vector.

## Cell Viability Assay

Cell viability and proliferation were determined with the EZ-Cytox Cell Viability Assay Kit (Daeil Labservice, Korea) based on the cleavage of the tetrazolium salt to water-soluble formazan by succinate-tetrazolium reductase. Briefly, 2 X $10^3$ of primary osteoblast precursors were seeded on 96-well plates and cultured for 24 hours. Then, cells were treated with trapidil and cultured in 200 μl of medium. After 1, 2, or 3 days of treatment, cells were incubated with

20 μl of Ez-CyTox solution for 2 hours in the 37°C incubator. Absorbance was measured at 450nm.

## Immunoblotting

Immunoblot analysis was performed as described previously (*45*). Specific antibodies against ALK3 and ALK2 (Santa Cruz Biotechnology, Santa Cruz, CA); phospho-Smad1/5/9, Smad1, phosphor-ERK, ERK, phosphor-JNK, JNK, phosphor-p38 and p38 (Cell Signaling Technology, Danvers, MA, USA); Runx2 (MBL, Nagoya, Japan); and β-actin (Sigma, St Louis, MO, USA) were used.

## Reverse transcription and real-time PCR analysis

Total RNA was prepared from cells or spleens by using an RNeasy Mini kit (Qiagen, Valencia, CA) according to the manufacturer's instructions, and cDNA was synthesized from 2 μg of total RNA by reverse transcriptase (Superscript II Preamplification System; Gibco-BRL, Gaithersburg, MD, USA). Real-time PCR was performed on an ABI Prism 7500 sequence detection system using a SYBR® Green PCR Master Mix (Applied Biosystems, Foster City, CA, USA) and following the manufacturer's protocols. The ABI 7500

sequence detector was programmed with the following PCR conditions: 40 cycles of 15-s denaturation at 95°C and 1-minute amplification at 60°C. All reactions were run in triplicate and normalized to the housekeeping gene β-actin. The evaluation of relative differences of PCR results was calculated by using the comparative cycle threshold ($C_T$) method. All of the primers used for RT-PCR are shown in Table 1.

## Statistical analysis

Data are presented as the mean ± SD (*in vitro* data) or the mean ± SEM (*in vivo* data). Statistical analysis was performed by either unpaired, two-tailed Student's *t* test or one-way ANOVA followed by Dunnett's test using GraphPad Prism 5.0 (GraphPad Software, San Diego, CA, USA). Values of $P < 0.05$ were considered significant. The data and statistical analyses comply with the recommendations on experimental design and analysis in pharmacology (*48*).

**Table 1. Primers for quantitative real-time PCR experiments**

| Gene | Forward (5’ -> 3’) | Reverse (3’ -> 5’) |
|---|---|---|
| *Tnap* | CAC ATA TCA AGG ATA TCG ACG TGA | ACA TCA GTT CTG TTC TTC GGG TAC A |
| *Runx2* | CGC ACG ACA ACC GCA CCA T | CAG CAC GGA GCA CAG GAA GTT |
| *Col1a1* | AAA CTC CCT CCA CC CCC TTC TCA | TT GGG TTG TTC GTC TGT TTC C |
| *Osx* | AGC ACC AAT GGC CAA TCT | AGG GTG GGT AGT CAT TTG CAT AG |
| *Bgalp2* | GGG CAA TAA GGT AGT GAA CAG | GCA GCA CAG GTC CTA AAT AGT |
| *Bsp* | CCG GCC ACG CTA CTT TCT T | TGG ACT GGA AAC CGT TTC AGA |
| *Id1* | GGT GGT ACT TGG TCT GTC GG | AGC CGT TCA TGT CGT AGA GC |
| *ALK2* | GTG GGA GAC AGC ACT CTA GC | CTT CCC GAC ACA CTC CAA CA |
| *ALK3* | GCA AGG ATT CAC CGA AAG CC | GCT GCC ATC AAA GAA CGG AC |
| *Bmp2* | GAA CTC TGT GAA TTC CAA AAT CCC T | TTT TTC CAT TCC ATT CCA TAA A |
| *Bmp4* | GGT AGA GGG GTG TGG ATG CC | CAA TAT GGT CAA AAC ATT TGC ACG |
| *Bmp7* | CTT CGA CGA CAG CTC TAA TGT CA | CGT CAC GTG CCA GAA GGA AA |
| *Actb* | ATG TGG ATC AGC AAG CAG GA | AAG GGT GTA AAA CGC AGC TC |

## Results

## Trapidil promotes bone regeneration *in vivo*

To investigate the effect of trapidil on the anabolic capacity to repair bone defects *in vivo*, a critical-size rat calvarial defect model was used (*45*). Eight-millimeter holes were drilled in the rat calvariae, and then they were covered with collagen sponges containing phosphate-buffered saline (PBS), trapidil, or recombinant human BMP2 (rhBMP2). The calvariae were analyzed using micro-computed tomography (μCT) 3 weeks after the surgery. The calvarial defect was significantly repaired by treatment with trapidil, similar to the bone anabolic effect of rhBMP2 and in contrast to PBS treatment (Figure 4). Histological analysis using hematoxylin and eosin (H&E) or Masson-Goldner trichrome staining and histomorphometry further confirmed the bone regeneration in the trapidil-treated groups was greater than that in the control groups (Figure 5). These data demonstrate that trapidil has bone anabolic capacity *in vivo*.

A

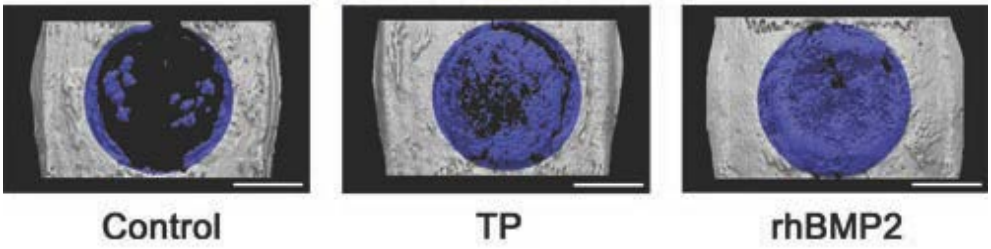


B

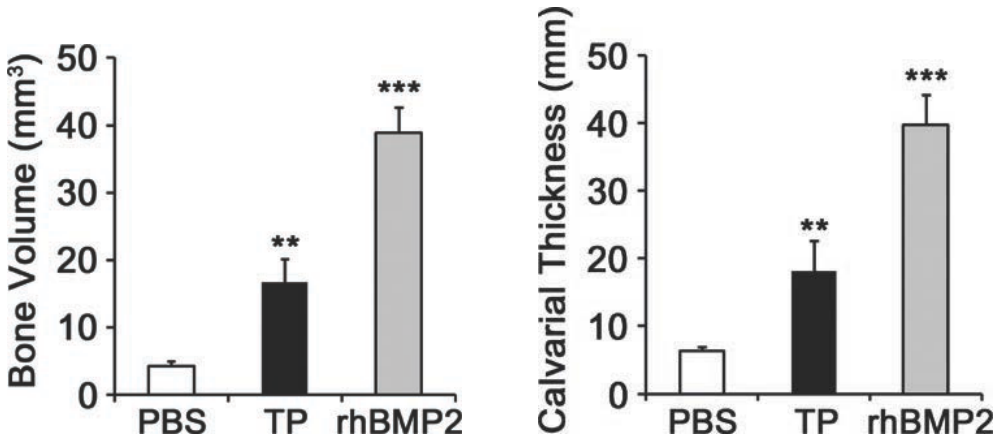


**Figure 4. Trapidil promotes bone regeneration**

(A,B) Critical-size rat calvarial defects were implanted with absorbable collagen sponges treated with PBS (control), trapidil (4 mg per scaffold), or rhBMP2 (2 μg per scaffold). (A) 3D μCT images. Scale bar, 4 mm. (B) Bone volume in the region of the defects (*left panel*) and calvarial thickness of new bone (*right panel*). In panel B, the bone volume and thickness were measured within the areas of the defects visualized in blue. Data represent mean ± SEM

(n = 6 for each experimental group). **P < 0.01; ***P< 0.001 *vs.* PBS-treated control by one-way ANOVA followed by Dunnett's test.

A

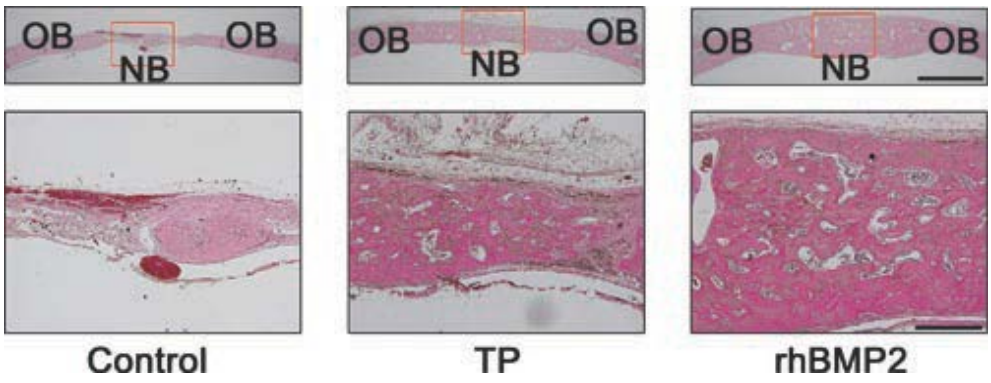


B

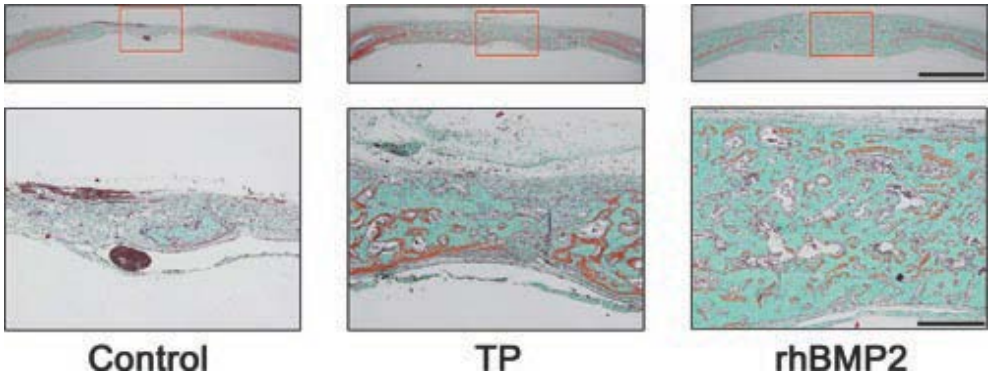


**Figure 5. Histology analysis of calvariae**

(A) H&E staining of rat calvarial sections. Scale bar, 2 mm (*upper panel*) and 200 μm (*bottom panel*). NB, new bone; OB, old bone (B) Masson's trichrome staining of rat calvarial sections to visualize mineralized bone. Scale bar, 2 mm (*upper panel*) and 200 μm (*bottom panel*). The results shown are representative of six independent samples.

## Trapidil enhances osteogenic differentiation *in vitro*

To investigate whether trapidil has bone anabolic effects *in vitro*, primary osteoblast precursors from mouse calvaria were isolated and then cultured with different concentrations of trapidil in osteogenic differentiation medium. Trapidil greatly enhanced alkaline phosphatase (ALP) staining (Figure 6A, *upper panel*), ALP activity (Figure 6B, *left panel*), *TNAP* expression (Figure 6B, *right panel*), and calcium deposition (Figure 6A, *bottom panel*) in a dose-dependent manner. Enhanced ALP staining and calcium deposition were also observed in a mouse MC3T3-E1 osteoblast cell line, mouse C2C12 myoblast cell line, or mouse bone marrow stromal cells (BMSCs, (Figure 7 A–C). In addition, the mRNA and protein expression of Runx2, a crucial transcription factor for the differentiation of osteoblasts, were elevated by trapidil (Figure 8). Furthermore, the mRNA expression of osteoblastic differentiation marker genes including *Col1a1*, *Osx*, *Bgalp2*, and *BSP* was increased by trapidil without affecting cell viability (Figure 9). However, cells exposed to 10 times higher concentration of trapidil (2 mM) showed less mineralization, although they showed higher ALP activity than cells exposed to 200 μM did (Figure 10A and B). In addition, cells treated with 2 mM trapidil showed inhibition of cell proliferation (Figure 10C). These *in vitro* results

demonstrate that trapidil directly promoted osteogenic differentiation of osteoblastic cells without affecting cell viability at concentrations up to 400 μM.

A

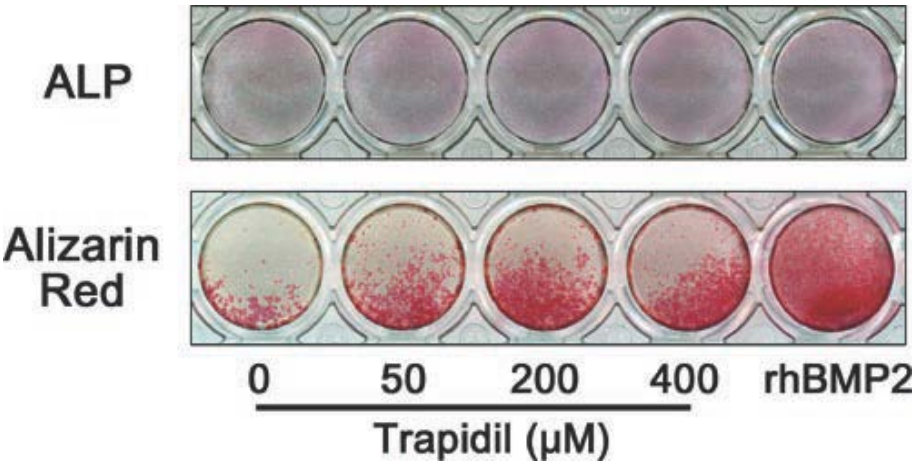


B

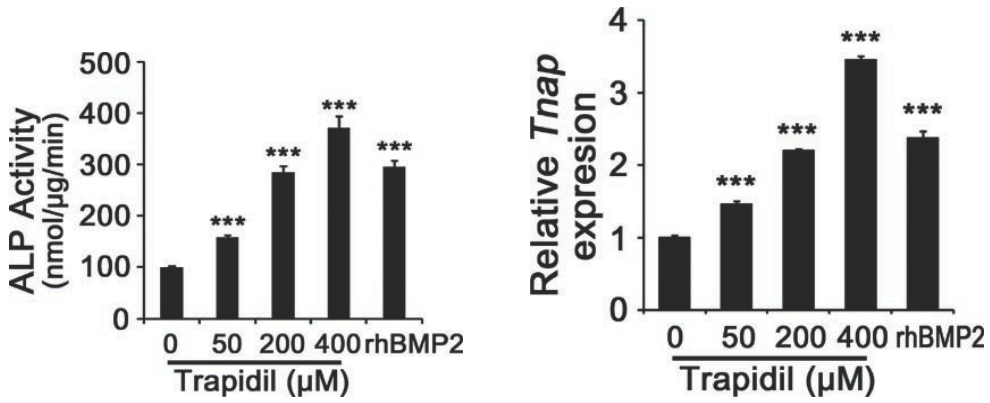


**Figure 6. Trapidil enhances osteogenic differentiation of calvarial osteoblast precursors**

(A,B) Mouse calvarial osteoblast precursors were cultured in osteogenic medium with or without different concentration of trapidil (50-400 μM) or

rhBMP2 (100 ng/mL). ALP staining (A, *top panel*) and ALP activity assay in cell lysates (B, *left panel*) were assayed on day 3. Alizarin red S staining was performed on day 14 (A, *bottom panel*). *Tnap* mRNA expression (B, *right panel*) was analyzed by real-time PCR on day 2. rhBMP2 was used as positive control of osteogenic differentiation. The results shown are representative of three independent experiments (n=3), and the values are expressed as mean ± SD. ***P < 0.001 *vs.* untreated control by unpaired Student's *t* test.

A

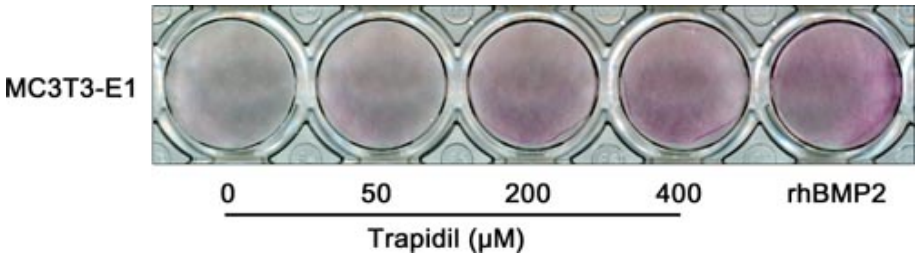


B

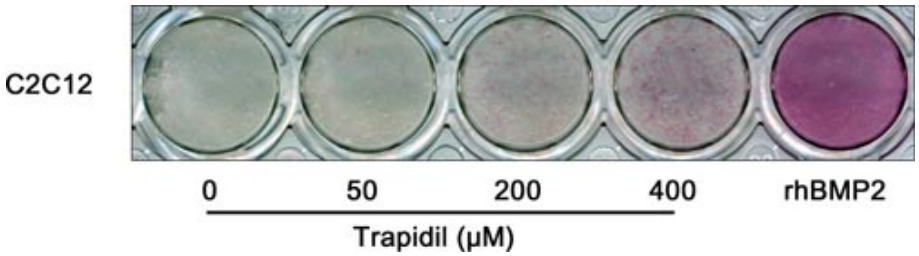


C

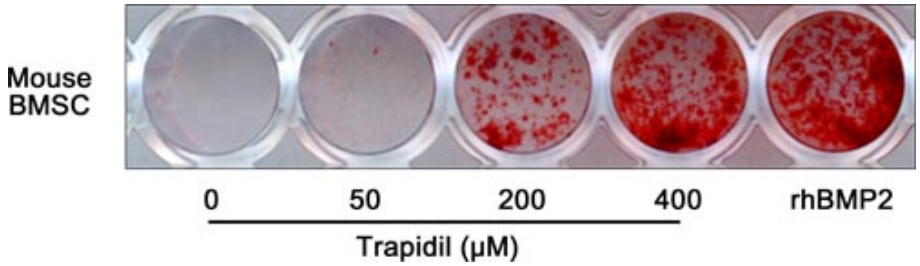


**Figure 7. Trapidil enhances osteogenic differentiation of osteoblastic cells**

(A-C) MC3T3-E1 cells, C2C12 cells, and mouse BMSCs were cultured in osteogenic medium with or without different concentration of trapidil (50-400 μM) or rhBMP2 (100 ng/mL). (A) ALP staining of MC3T3-E1 cells was performed on day 3. (B) ALP staining of C2C12 cells was performed on day 3.

(C) Alizarin red S staining of mouse BMSCs was performed on day 14. rhBMP2 was used as positive control of osteogenic differentiation. The results shown are representative of three independent experiments (n=3)

A

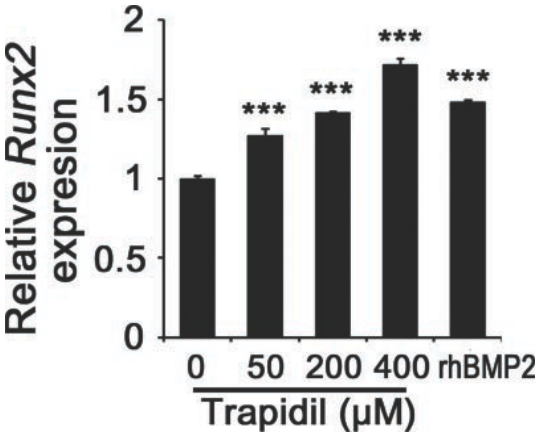


B

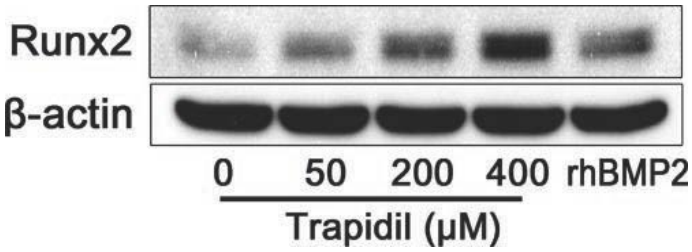


**Figure 8. Trapidil induces Runx2 expression**

(A,B) Mouse calvarial osteoblast precursors were cultured in osteogenic medium with or without different concentration of trapidil (50-400 μM) or rhBMP2 (100 ng/mL). (A) *Runx2* mRNA expression was analyzed by real-time PCR on day 2. (B) Whole-cell lysates were subjected to immunoblotting with the indicated antibodies on day 2. rhBMP2 was used as positive control of

osteogenic differentiation. The results shown are representative of three independent experiments (n=3), and the values are expressed as mean ± SD. ***P < 0.001 *vs.* untreated control by unpaired Student's *t* test.

A

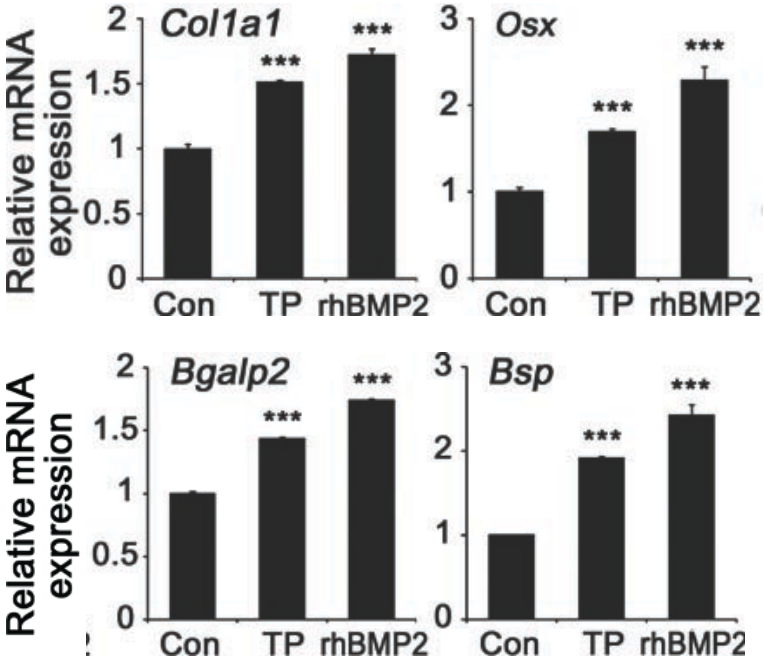


B

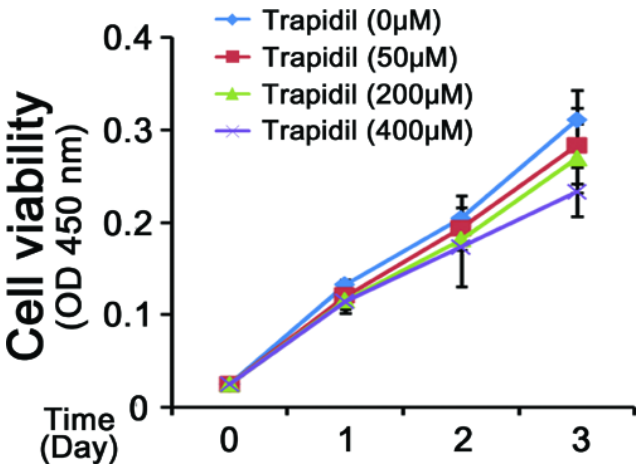


**Figure 9. Trapidil promotes expression of osteogenic genes**

(A) Mouse calvarial osteoblast precursors were cultured in osteogenic medium with trapidil (400 μM) or rhBMP2 (100 ng/mL). *Col1a1*, *Osx*, *Bgalp2*, and *Bsp* mRNA expression was analyzed by real-time PCR on day 2. (B) Mouse calvarial osteoblast precursors were cultured in osteogenic medium with or without different concentration of trapidil (50-400 μM) for the indicated times and then cell viabilities were measured. rhBMP2 was used as positive control of osteogenic differentiation. The results shown are representative of three independent experiments (n=3), and the values are expressed as mean ± SD. ***P < 0.001 *vs.* untreated control by unpaired Student's *t* test.

A

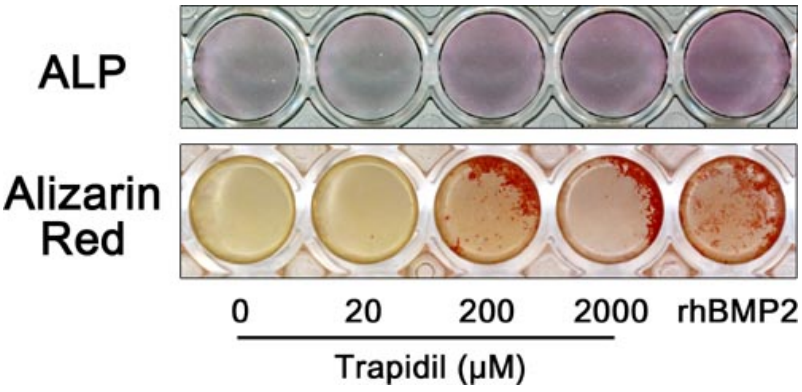
ALP
Alizarin Red
0
20
200
2000
rhBMP2
Trapidil (μM)

B

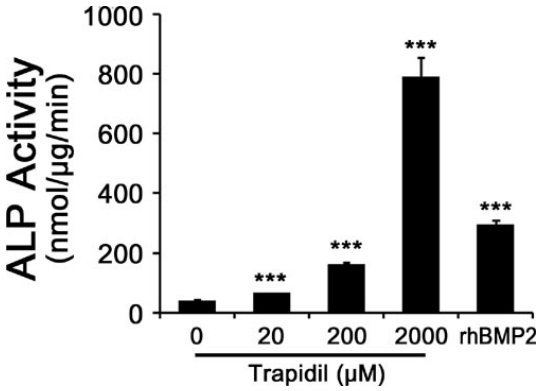
ALP Activity
(nmol/μg/min)
1000
800
600
400
200
0
***
***
***
***
0
20
200
2000
rhBMP2
Trapidil (μM)

C

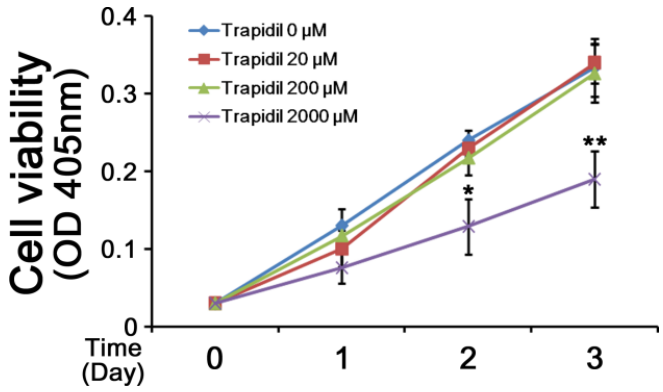
Cell viability
(OD 405nm)
0.4
0.3
0.2
0.1
0
Trapidil 0 μM
Trapidil 20 μM
Trapidil 200 μM
Trapidil 2000 μM
*
**
Time
(Day)
0
1
2
3

**Figure 10. High concentration of trapidil inhibited mineralization and cell proliferation**

(A,B) Mouse calvarial osteoblast precursors were cultured in osteogenic medium with or without different concentration of trapidil (20-2000 μM) or rhBMP2 (100 ng/mL). ALP staining (A, *top panel*) and ALP activity assay in cell lysates (B, *left panel*) were assayed on day 3. Alizarin red S staining was performed on day 14 (A, *bottom panel*). rhBMP2 was used as positive control of osteogenic differentiation. (C) Mouse calvarial osteoblast precursors were cultured in osteogenic medium with or without different concentration of trapidil (20-2000 μM) for the indicated times and then cell viabilities were measured. The results shown are representative of three independent experiments (n=3), and the values are expressed as mean ± SD. ***P < 0.001 *vs.* untreated control by unpaired Student's *t* test.

## Trapidil induces BMPR signaling

As trapidil upregulated Runx2 (Figure 7), the status of upstream effectors of Runx2 such as MAPKs, Akt, and Smad1/5/9 was examined. In addition, trapidil has been reported to activate protein kinase A (PKA), which also regulates the expression of Runx2 (*36, 49, 50*). Thus, the status of cAMP response element binding (CREB) protein, which is downstream of PKA was also examined. As shown in Figure 10A, trapidil greatly increased the phosphorylation of ERK, JNK, p38, Akt, and CREB. Notably, Smad1/5/9 phosphorylation was also increased by trapidil in mouse calvarial osteoblasts (Figure 11A) as well as MC3T3-E1 cells, C2C12 cells, and mouse BMSCs (Figure 12A–C, respectively). As a result, Id-1 mRNA expression (Figure 11B) and its promoter activity (Figure 11C) were increased by trapidil. However, the mRNA expression of BMPs expressed in osteoblast cells including *Bmp2*, *Bmp4*, and *Bmp7*, was not affected by trapidil (Figure 13).

To investigate whether BMPR activation is involved in the trapidil-induced osteogenesis, the cells were pretreated with LDN193189, a specific inhibitor of ALK2 and ALK3. In the presence of LDN193189, the trapidil-induced phosphorylation of Smad1/5/9 (Figure 14A), Runx2 protein expression (Figure 14B), ALP activity (Figure 14C), and calcium deposition (Figure 14D)

were nearly abolished. These results indicate that BMPR activation is required for trapidil-induced osteogenesis.

A

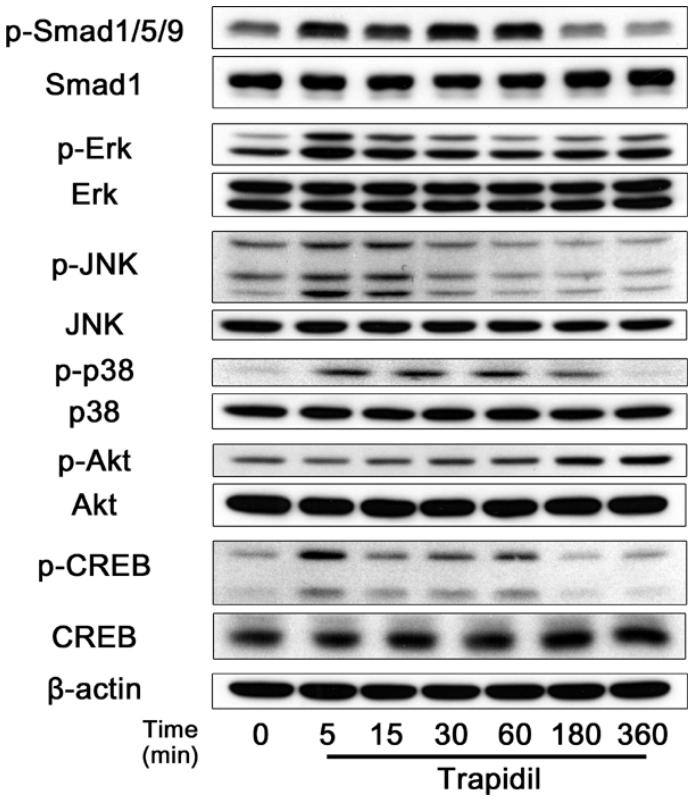
p-Smad1/5/9
Smad1
p-Erk
Erk
p-JNK
JNK
p-p38
p38
p-Akt
Akt
p-CREB
CREB
β-actin
Time (min)
0 5 15 30 60 180 360
Trapidil

B

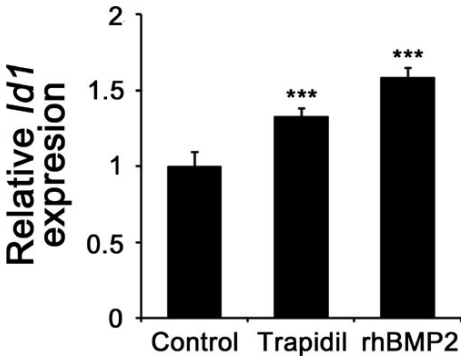
Relative Id1 expresion
2
1.5
1
0.5
0
***
***
Control
Trapidil
rhBMP2

C

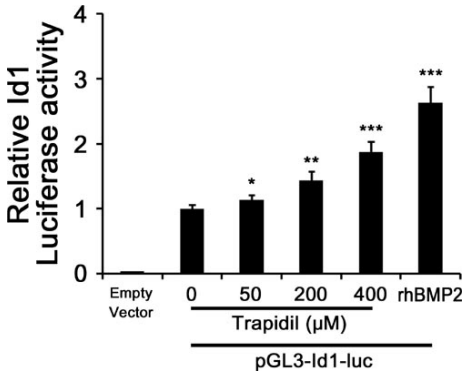
Relative Id1 Luciferase activity
4
3
2
1
0
*
**
***
***
Empty Vector
0
50
200
400
rhBMP2
Trapidil (μM)
pGL3-Id1-luc

**Figure 11. Trapidil induces phosphorylation of Smad1/5/9**

(A) Mouse calvarial osteoblast precursors were cultured with trapidil (400 μM) for the indicated times and then whole-cell lysates were subjected to immunoblotting with the indicated antibodies. (B) Mouse calvarial osteoblast precursors were cultured in osteogenic medium with trapidil (400 μM) or rhBMP2 (100 ng/ml) for 12h. *Id1* mRNA expression was analyzed by real-time PCR. (C) Mouse calvarial osteoblast precursors were electroporated with or without pGL3-Id1-luc vector. The cells were treated with or without different concentrations of trapidil (50-400 μM) or rhBMP2 (100 ng/mL) for 24 hours and promoter activity was analyzed by luciferase reporter assay. . rhBMP2 was used as positive control of osteogenic differentiation. The results shown are representative of three independent experiments (n=3), and the values are expressed as mean ± SD. *P < 0.05; **P < 0.01; ***P < 0.001 *vs.* untreated control by unpaired Student's *t* test.

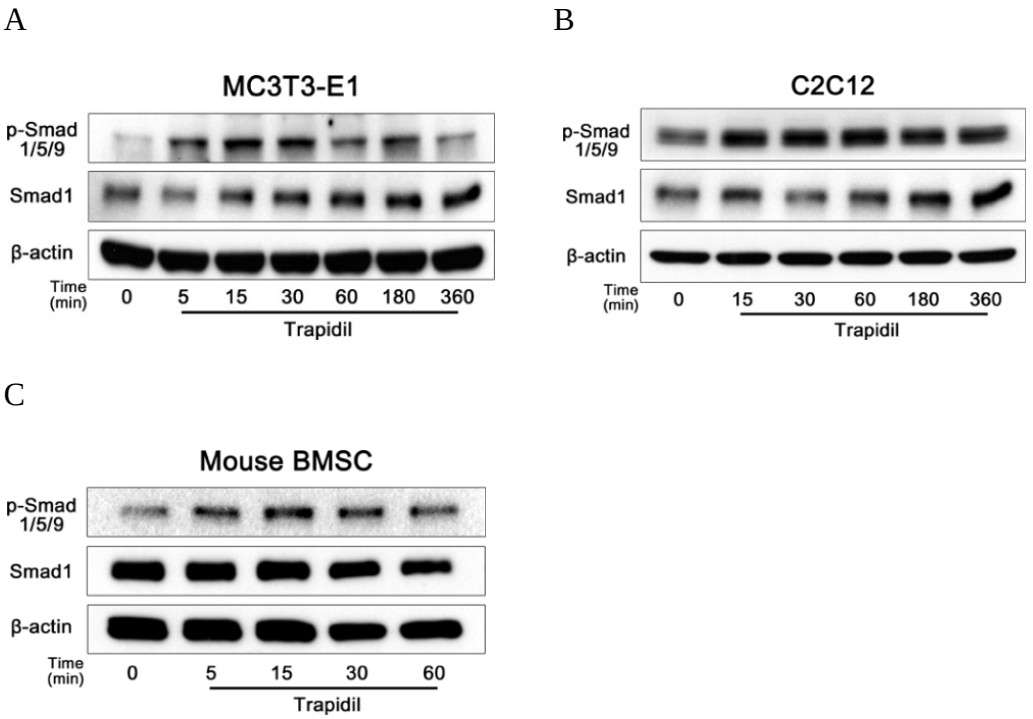


**Figure 12. Trapidil enhances phosphorylation of Smad1/5/9 in MC3T3-E1 cells, C2C12 cells and mouse BMSCs**

(A) MC3T3-E1 cells were treated with trapidil (400 μM) for the indicated times and then whole-cell lysates were subjected to immunoblotting with the indicated antibodies. (B) C2C12 cells were treated with trapidil (400 μM) for the indicated times and then whole-cell lysates were subjected to immunoblotting with the indicated antibodies. (C) Mouse BMSCs were treated with trapidil (400 μM) for the indicated times and then whole-cell lysates were

subjected to immunoblotting with the indicated antibodies. The results shown are representative of three ind0ependent experiments (n=3).

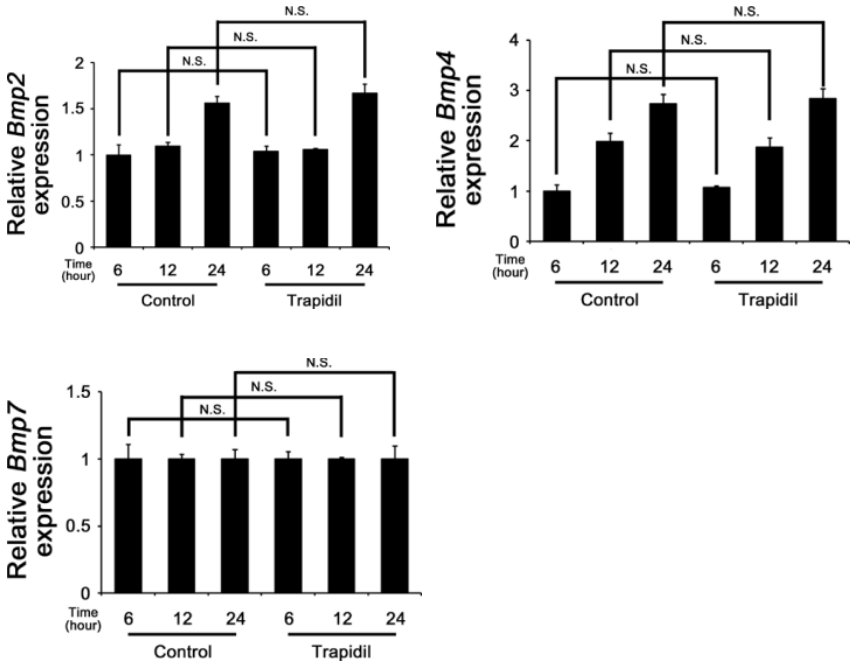


**Figure 13. Trapidil does not affect the expression of BMPs**

Mouse calvarial osteoblast precursors were cultured in osteogenic medium with trapidil (400 μM) for the indicated times and then *Bmp2*, *Bmp4*, and *Bmp7* mRNA expression was analyzed by real-time PCR. The results shown are representative of three independent experiments (n=3), and the values are expressed as mean ± SD. N.S. Not significant

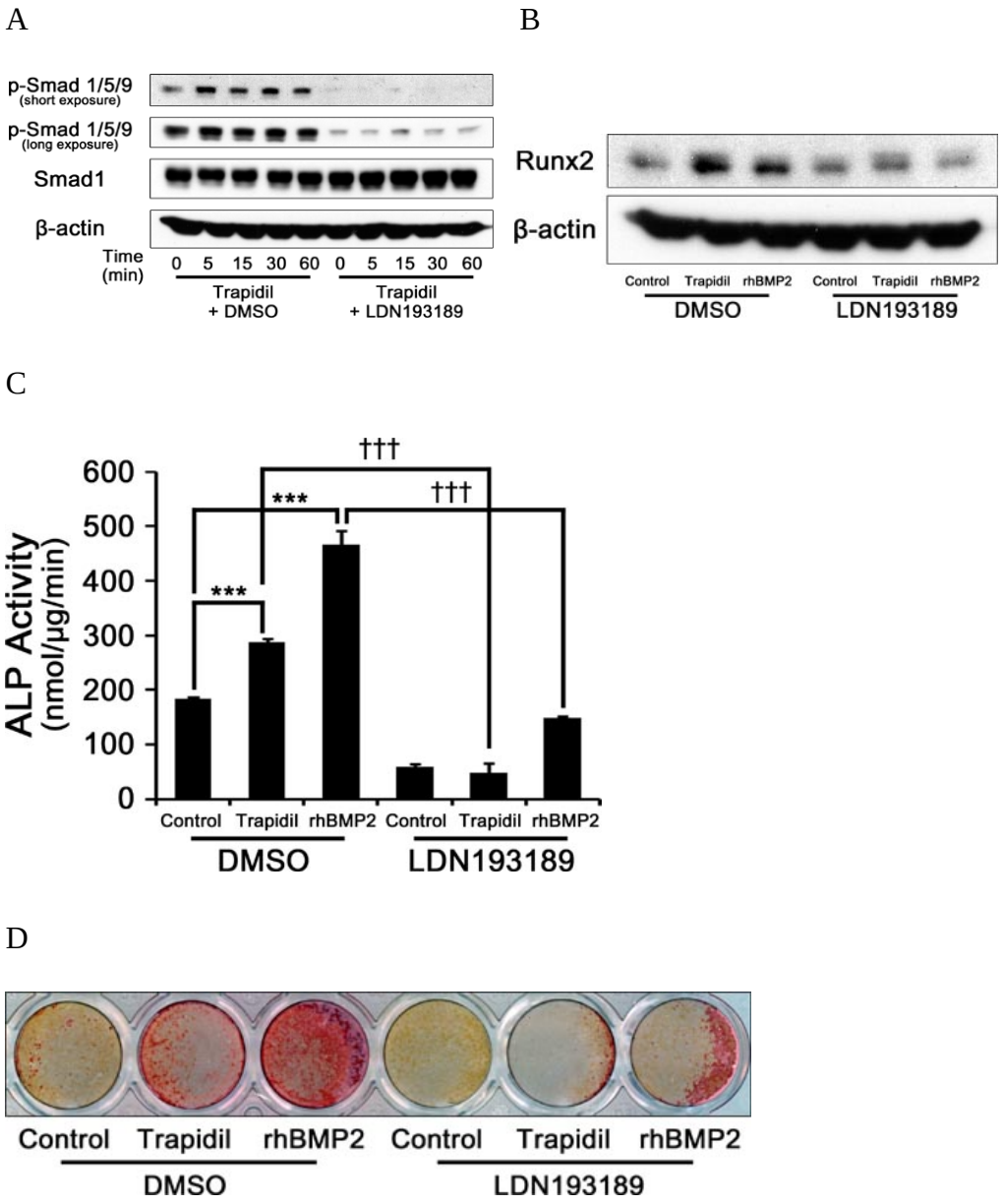


**Figure 14. LDN193189 inhibits trapidil-induced osteogenesis**

(A) Mouse calvarial osteoblast precursors were pretreated with DMSO or

LDN193189 (100 nM) and then treated with trapidil (400 μM) for the indicated times. Whole-cell lysates were subjected to immunoblotting with the indicated antibodies. (B-D) Mouse calvarial osteoblast precursors were cultured in osteogenic medium with PBS, trapidil (400 μM) or rhBMP2 (100 ng ng/mL) in the presence or absence of LDN193189 (100 nM). (B) Whole-cell lysates were subjected to immunoblotting with the indicated antibodies on day 2. (C) ALP activity assay in cell lysates was assayed on day 3. (D) Alizarin red S staining was performed on day 14. The results shown are representative of three independent experiments (n=3), and the values are expressed as mean ± SD. ***P < 0.001 *vs.* untreated control by unpaired Student's *t* test. †††P < 0.001 *vs.* each trapidil- or BMP2-treated sample without LDN193189 by unpaired Student's *t* test.

## Inhibition of PDGF signaling induces BMP signaling

Next, we investigated whether trapidil induced osteogenesis by inhibiting PDGF signaling using other known PDGFR inhibitors, imatinib, PDGFR inhibitor IV, and PDGFR inhibitor V. Similar to trapidil, the imatinib, PDGFR inhibitor IV, and PDGFR inhibitor V also increased osteogenic differentiation (Figure 15A–C). Moreover, phosphorylation of Smad1/5/9 was also enhanced by imatinib, PDGFR inhibitor IV, and PDGFR inhibitor V (Figure 16A–C), indicating that inhibition of PDGF signaling activated BMP signaling pathways and subsequently promoted osteogenesis. Therefore, trapidil activated BMP signaling-related mediators by inhibiting PDGF signaling.

A

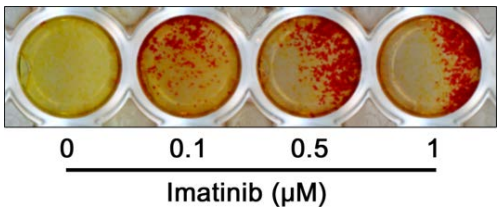


B

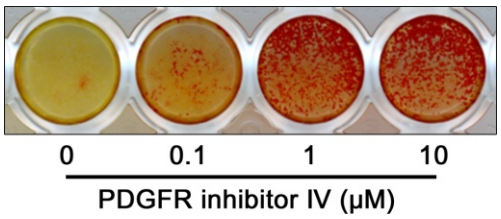


C

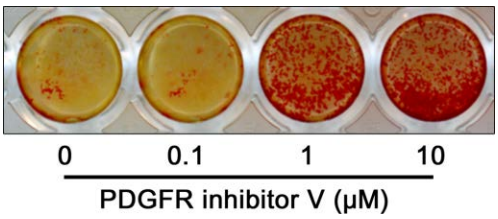


**Figure 15. Inhibition of PDGFR promotes osteogenesis**

(A) Mouse calvarial osteoblast precursors were cultured in osteogenic medium with or without different concentrations of imatinib (0.1-1 μM) for 14 days and then alizarin red S staining was performed. (B) Mouse calvarial osteoblast precursors were cultured in osteogenic medium with or without different concentrations of PDGFRi IV (0.1-10 μM) for 14 days and then alizarin red S staining was performed. (C) Mouse calvarial osteoblast precursors were cultured in osteogenic medium with or without different concentrations of PDGFRi V (0.1-10 μM) for 14 days and then alizarin red S staining was performed. The results shown are representative of three independent

experiments (n=3).

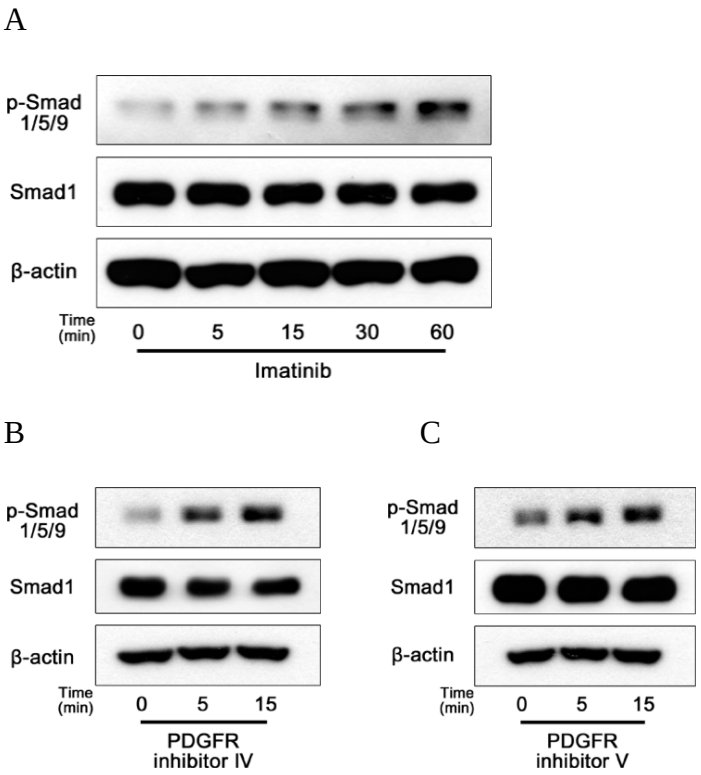


**Figure 16. Inhibition of PDGFR promotes phosphorylation of Smad1/5/9**

(A) Mouse calvarial osteoblast precursors were treated with imatinib (1 μM) for the indicated times and then whole-cell lysates were subjected to immunoblotting with the indicated antibodies. (B) Mouse calvarial osteoblast precursors were treated with PDGFRi IV (2 μM) for the indicated times and then whole-cell lysates were subjected to immunoblotting with the indicated antibodies. (C) Mouse calvarial osteoblast precursors were treated with PDGFRi V (2 μM) for the indicated times and then whole-cell lysates were

subjected to immunoblotting with the indicated antibodies The results shown are representative of three independent experiments (n=3).

## ALK3 is required for the trapidil-induced osteogenesis

To determine the involvement of ALK2 or ALK3 in trapidil-induced osteogenesis, ALK2 or ALK3 was depleted by transfecting mouse calvarial osteoblasts cells with the corresponding short hairpin RNA (shRNA)-containing lentivirus. Specific depletion of ALK3 (Figure 17A) significantly inhibited the trapidil-induced phosphorylation of Smad1/5/9 (Figure 18A), Runx2 protein expression (Figure 18B), ALP activity (Figure 18C), and calcium deposition (Figure 18D). However, ALK2 depletion caused a slight increase in basal ALK3 protein expression (Figure 17B). Smad1/5/9 phosphorylation (Figure 19A), Runx2 protein expression (Figure 19B), ALP activity (Figure 19C), and calcium deposition (Figure 19D) were also slightly increased with increasing levels of ALK3 induced by shALK2. These data demonstrate that ALK3 was involved in the trapidil-induced osteogenesis.

A

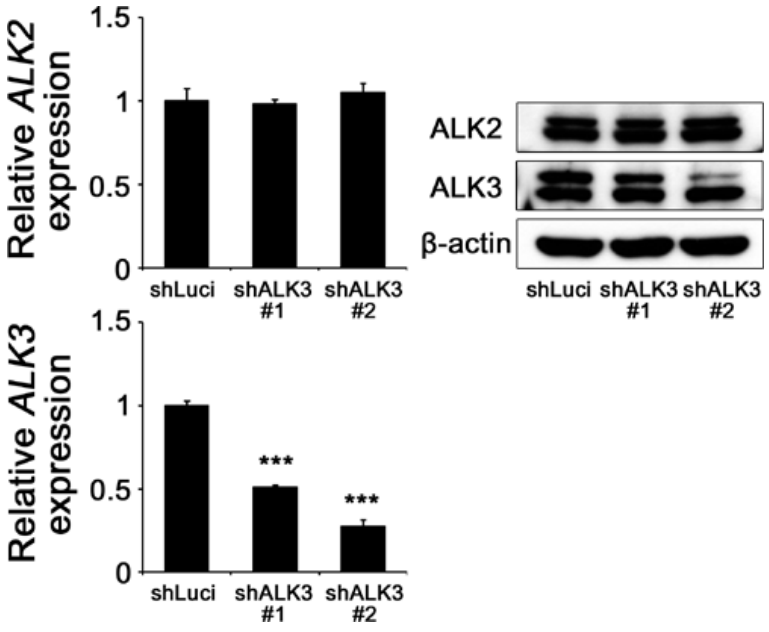
Relative ALK2 expression
1.5
1
0.5
0
shLuci
shALK3 #1
shALK3 #2
ALK2
ALK3
β-actin
shLuci shALK3 #1 shALK3 #2
Relative ALK3 expression
1.5
1
0.5
0
***
***
shLuci
shALK3 #1
shALK3 #2

B

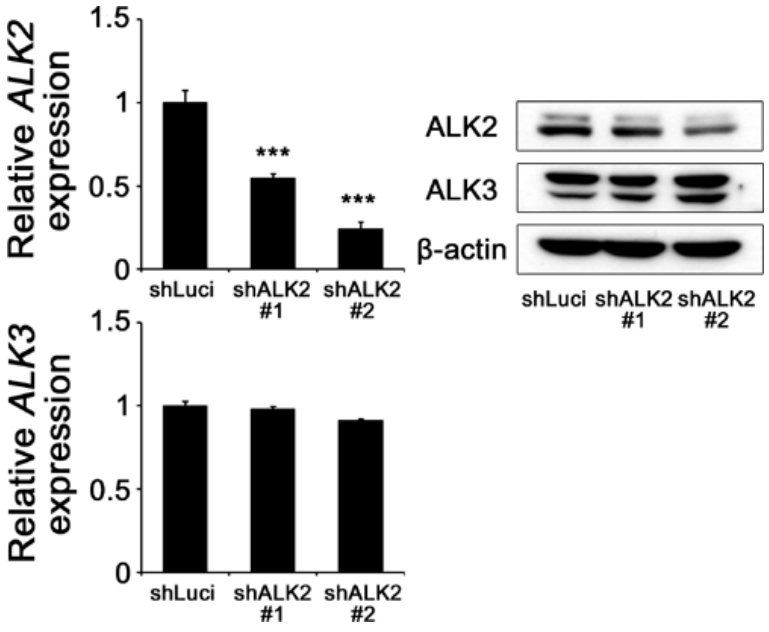
Relative ALK2 expression
1.5
1
0.5
0
***
***
shLuci
shALK2 #1
shALK2 #2
ALK2
ALK3
β-actin
shLuci shALK2 #1 shALK2 #2
Relative ALK3 expression
1.5
1
0.5
0
shLuci
shALK2 #1
shALK2 #2

**Figure 17. Depletion of ALK2 or ALK3**

(A) Mouse calvarial osteoblast precursors were infected with lenti viruses containing shLuci or two kinds of shALK3. *ALK2* and *ALK3* mRNA expression was analyzed by real-time PCR (*left panel*). Whole-cell lysates were subjected to immunoblotting with the indicated antibodies (*right panel*). (B) Mouse calvarial osteoblast precursors were infected with lenti viruses containing shLuci or two kinds of shALK2. *ALK2* and *ALK3* mRNA expression was analyzed by real-time PCR (*left panel*). Whole-cell lysates were subjected to immunoblotting with the indicated antibodies (*right panel*). The results shown are representative of three independent experiments (n=3), and the values are expressed as mean ± SD. ***P < 0.001 *vs.* control with shLuci by unpaired Student's *t* test. †††P < 0.001 *vs.* trapidil-treated sample with shLuci by unpaired Student's *t* test.

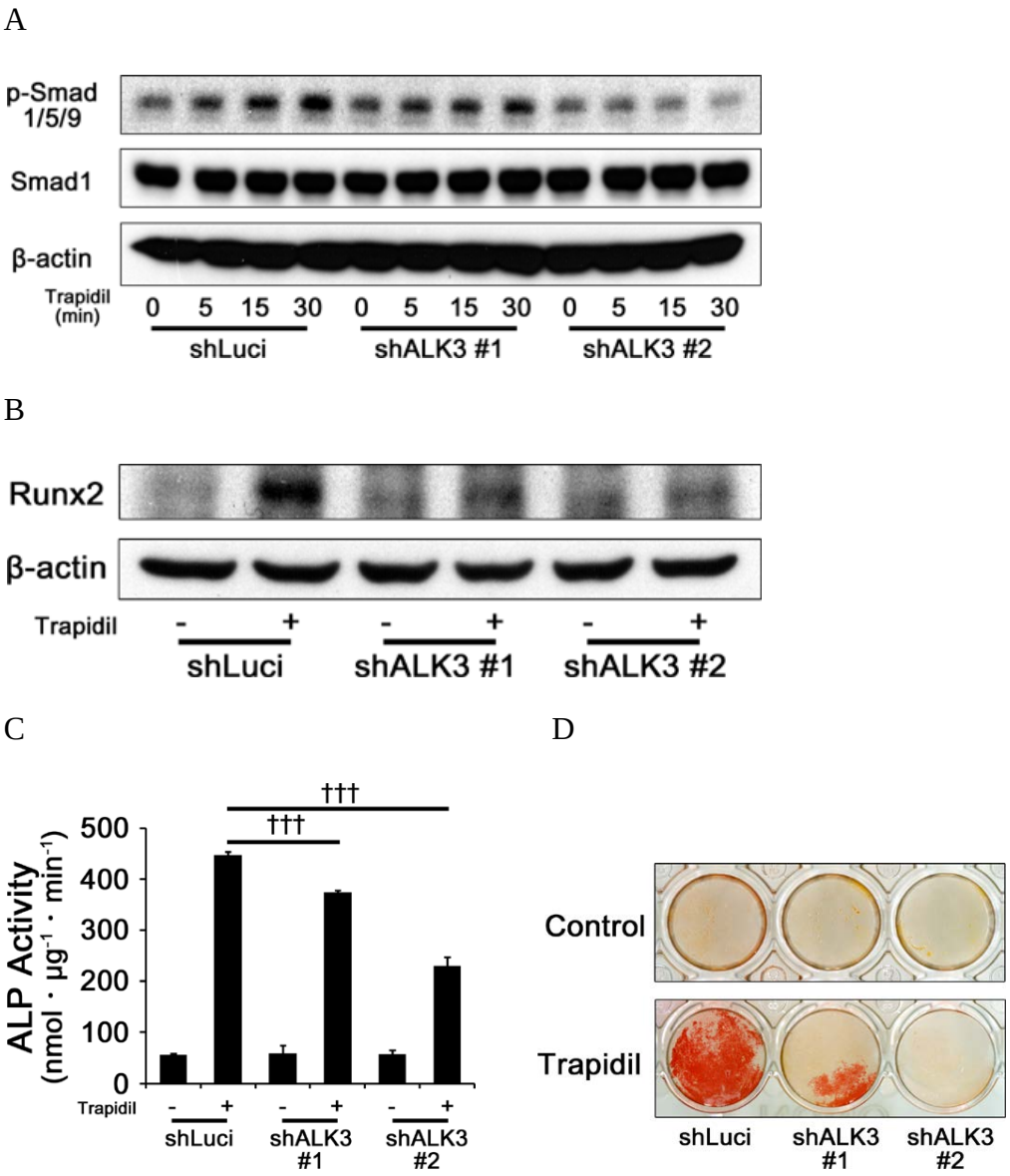


**Figure 18. ALK3 is required for the trapidil-induced osteogenesis**

Mouse calvarial osteoblast precursors were infected with lenti viruses containing shLuci or two kinds of shALK3. (A) The cells were treated with trapidil for the indicated times. Whole-cell lysates were subjected to immunoblotting with the indicated antibodies. (B) The cells were treated with or without trapidil (400 μM) for 48 hours. Whole-cell lysates were subjected to immunoblotting with the indicated antibodies. (C) The cells were cultured with or without trapidil (400 μM) for 3 days and ALP activity in cell lysates was assayed. (D) The cells were cultured with or without trapidil (400 μM) for 14 days and then alizarin red S staining was performed. The results shown are representative of three independent experiments (n=3), and the values are expressed as mean ± SD. †††$P < 0.001$ *vs.* trapidil-treated sample with shLuci by unpaired Student's *t* test.

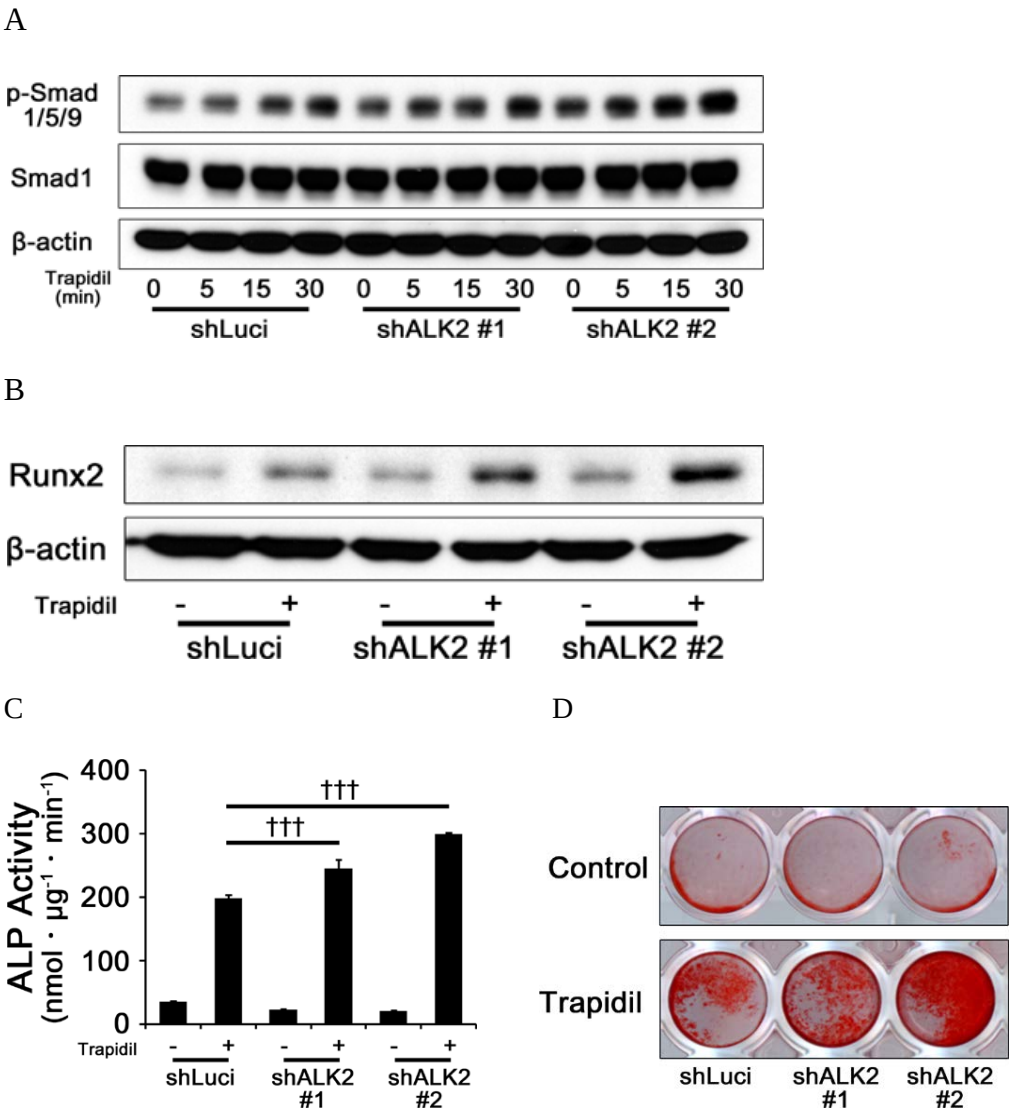


**Figure 19. ALK2 is not involved in trapidil-induced osteogenesis**

Mouse calvarial osteoblast precursors were infected with lenti viruses containing shLuci or two kinds of shALK2. (A) The cells were treated with

trapidil for the indicated times. Whole-cell lysates were subjected to immunoblotting with the indicated antibodies. (B) The cells were treated with or without trapidil (400 μM) for 48 hours. Whole-cell lysates were subjected to immunoblotting with the indicated antibodies. (C) The cells were cultured with or without trapidil (400 μM) for 3 days and ALP activity in cell lysates was assayed. (D) The cells were cultured with or without trapidil (400 μM) for 14 days and then alizarin red S staining was performed. The results shown are representative of three independent experiments (n=3), and the values are expressed as mean ± SD. †††P < 0.001 *vs.* trapidil-treated sample with shLuci by unpaired Student's *t* test.

## Trapidil induces BMP-mediated BMPR activity

Next, the mechanism by which trapidil induces BMPR activity were investigated. Although trapidil did not affect the expression of BMPs (Figure 13), the possibility that autocrine BMP signaling was involved in the trapidil-induced osteogenesis could not be ruled out. Therefore, the culture medium was replaced with fresh medium immediately before trapidil treatment to minimize the autocrine BMP signaling. The result showed that the phosphorylation of Smad1/5/9 was not altered by trapidil (Figure 20), indicating that trapidil did not directly activate BMPR and autocrine BMP signaling was required for the trapidil-induced activation of BMPR. In addition, the trapidil-induced Smad1/5/9 phosphorylation (Figure 21A), Runx2 protein expression (Figure 21B), ALP activity (Figure 21C), and calcium deposition (Figure 21D) were greatly blocked in the presence of noggin, an antagonist of several BMPs. Notably, trapidil showed a synergistic effect with exogenous cotreatment with BMP2 to increase the Smad1/5/9 phosphorylation (Figure 22A), Runx2 protein expression (Figure 22B), and calcium deposition (Figure 22C). Together, these data demonstrate that trapidil induced autocrine BMP signaling or exogenous BMP2 signaling, which promoted BMPR activity and osteogenesis.

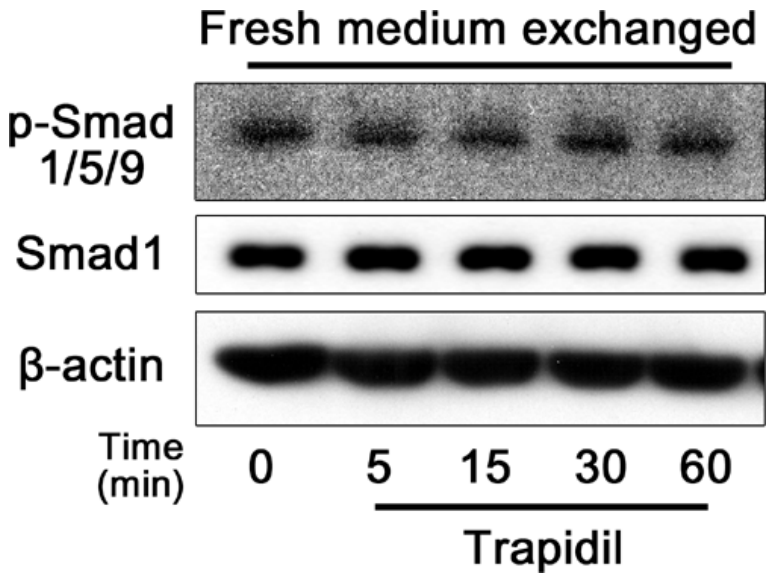


**Figure 20. Trapidil does not induce phosphorylation of Smad1/5/9 under autologous BMP-free condition**

Mouse calvarial osteoblast precursors were serum-starved for 12 hours and then exchanged with fresh serum-free medium. After 20 minutes of culture with the fresh-medium, cells were treated with trapidil (400 μM) for the indicated times and then whole-cell lysates were subjected to immunoblotting with the indicated antibodies. The results shown are representative of three independent experiments (n=3)

A

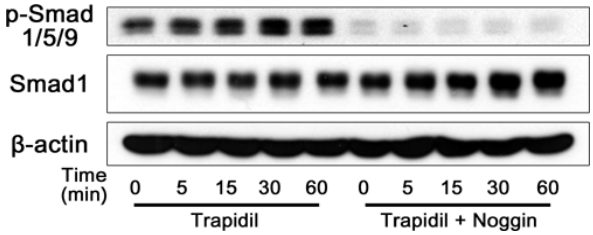
p-Smad 1/5/9
Smad1
β-actin
Time (min)
0 5 15 30 60 0 5 15 30 60
Trapidil
Trapidil + Noggin

B

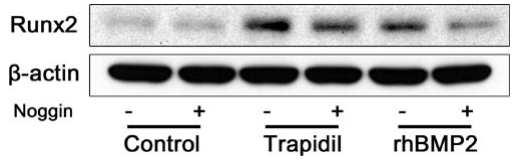
Runx2
β-actin
Noggin
- + - + - +
Control
Trapidil
rhBMP2

C

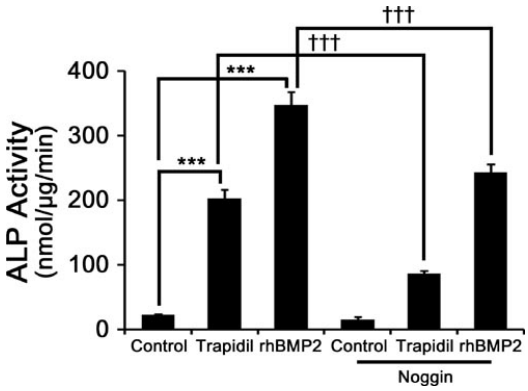
ALP Activity (nmol/μg/min)
400
300
200
100
0
***
***
†††
†††
Control Trapidil rhBMP2 Control Trapidil rhBMP2
Noggin

D

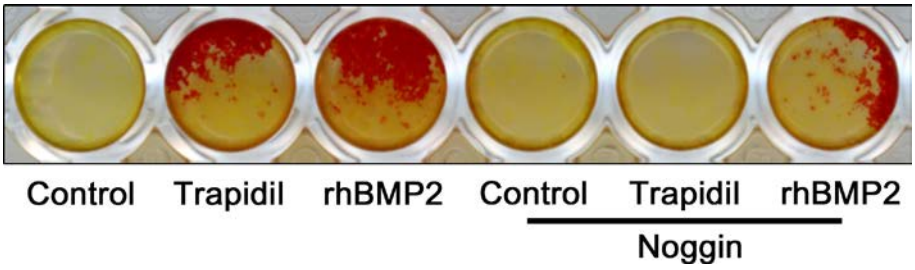
Control
Trapidil
rhBMP2
Control
Trapidil
rhBMP2
Noggin

**Figure 21. Noggin inhibits trapidil-mediated osteogenesis**

(A) Mouse calvarial osteoblast precursors were pretreated with or without noggin (100 ng/mL) for 4 hours. The cells were treated with trapidil (400 μM) for the indicated times and then whole-cell lysates were subjected to immunoblotting with the indicated antibodies. (B-C) Mouse calvarial osteoblast precursors were cultured in osteogenic medium with PBS, trapidil (400 μM) or rhBMP2 (100 ng/mL) in the presence or absence of noggin (100 ng/mL). (B) Whole-cell lysates were subjected to immunoblotting with the indicated antibodies on day 2. (C) ALP activity in cell lysates was assayed on day 3. (D) Alizarin red S staining was performed on day 14. The results shown are representative of three independent experiments (n=3), and the values are expressed as mean ± SD. ***P < 0.001 *vs.* control by unpaired Student's *t* test. †††P < 0.001 *vs.*teach trapidil- or BMP2-treated sample without noggin by unpaired Student's *t* test.

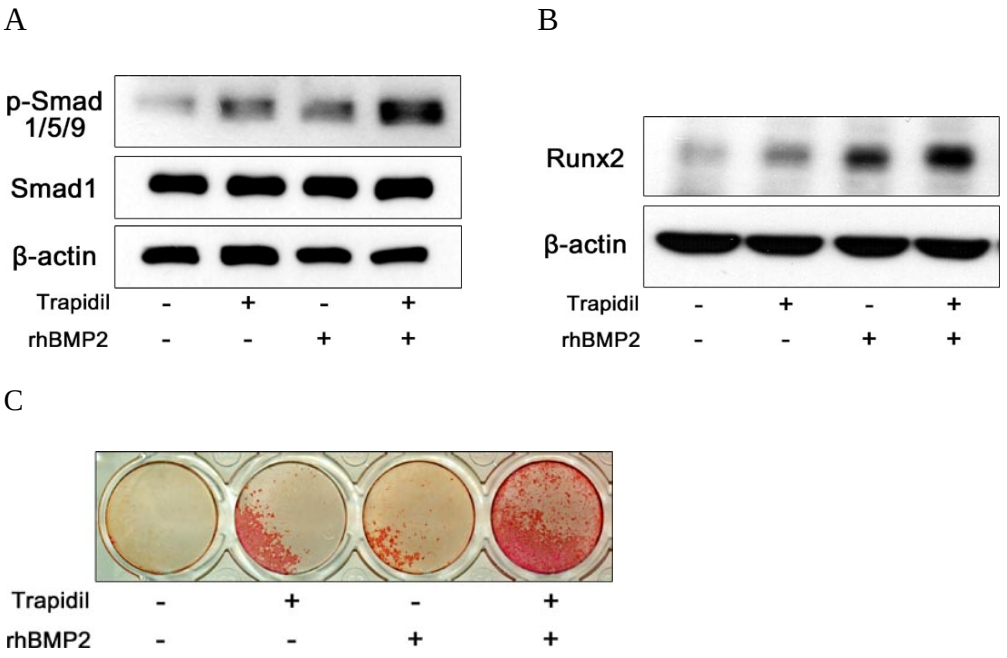


**Figure 22. Trapidil synergistically induces osteogenesis with BMP2**

(A) Mouse calvarial osteoblast precursors were treated with trapidil (400 μM) in the presence or absence of rhBMP2 (10 ng/mL) for 30 minutes and then whole-cell lysates were subjected to immunoblotting with the indicated antibodies. (B, C) Mouse calvarial osteoblast precursors were cultured in osteogenic medium with trapidil (400 μM) in the presence or absence of rhBMP2 (10 ng/mL). (B) Whole-cell lysates were subjected to immunoblotting with the indicated antibodies on day 2. (C) Alizarin red S staining was performed on day 14. The results shown are representative of three independent experiments (n=3).

## Akt but not CREB is involved in trapidil-induced osteogenesis

Akt is also activated by BMPs and promotes BMP-induced osteogenesis. (*51-53*). Previously, trapidil also activated Akt (Figure 11). Thus, we investigated whether trapidil-induced Akt is involved in trapidil-promoted osteogenesis by transfecting of wild-type (WT) Akt and Kinase-dead (KD)-Akt (a dominant negative mutant) constructs into calvarial osteoblast precursors (Figure 23). As shown in Figure 24, trapidil-induced ALP staining (Figure 24A, *upper panel*), ALP activity (Figure 24B), and mineralization (Figure 24A, *bottom panel*) were decreased more in cells with KD-Akt than they were in cells with WT-Akt. Trapidil-increased Runx2 expression was also inhibited in cells with KD-Akt (Figure 24C). These data suggest that Akt is also involved in trapidil-induced osteogenic differentiation.

A previous study has shown that trapidil activates PKA signaling pathway (*36*). Consistent with this report, trapidil induced phosphorylation of CREB, a direct downstream molecule of PKA (Figure 11). PKA/CREB signaling is involved in osteogenic differentiation (*54*). Therefore, we investigated whether trapidil-induced CREB is involved in trapidil-enhanced osteogenesis using various CREB constructs: WT-CREB, the phosphorylation defective mutant of CREB at serine 133 (S133A-CREB), and a DNA binding

domain mutant of CREB (K-CREB). Calvarial osteoblast precursors were transfected with a retrovirus containing CREB constructs (Figure 25), which promoted osteogenic differentiation. As shown in Figure 26, trapidil-induced ALP staining (Figure 26A, *upper panel*), ALP activity (Figure 26B), and mineralization (Figure 26A, *bottom panel*) were unchanged in cells with both S133A-CREB and K-CREB. Trapidil-induced Runx2 expression was also unaffected by transfection with S133A-CREB and K-CREB (Figure 26C). These data indicate that trapidil-activated CREB was not involved in trapidil-induced osteogenesis.

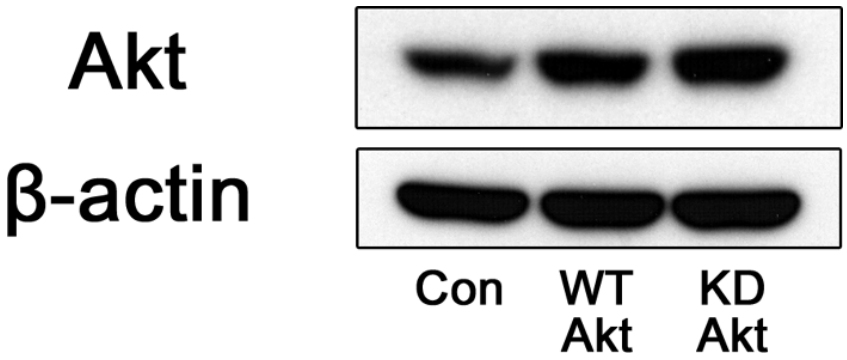


**Figure 23. Overexpression of Akt constructs in calvarial osteoblasts**

Mouse calvarial osteoblast precursors were electroporated with vectors which are pMSCV empty vector; control vector, pMSCV-Akt-WT, and pMSCV-Akt-KD. The cells were cultured for 24 hours after electroporation and then whole-cell lysates were subjected to immunoblotting with the indicated antibodies. The results shown are representative of three independent experiments (n=3).

A

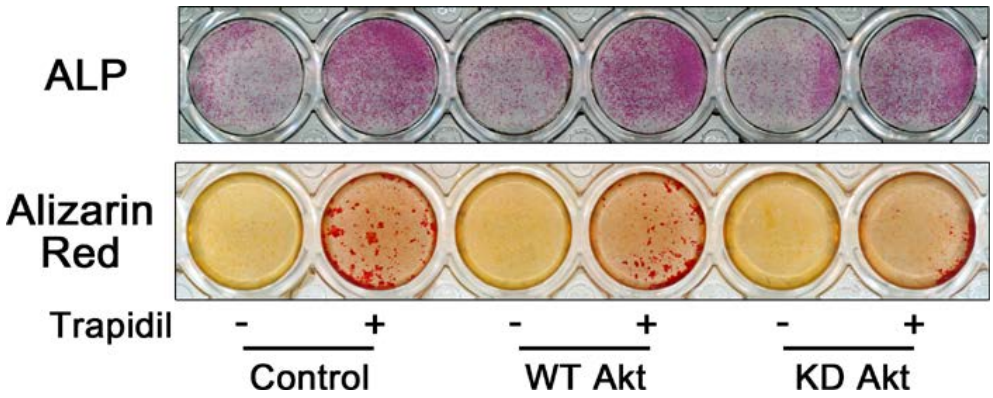
ALP
Alizarin Red
Trapidil
-
+
-
+
-
+
Control
WT Akt
KD Akt

B

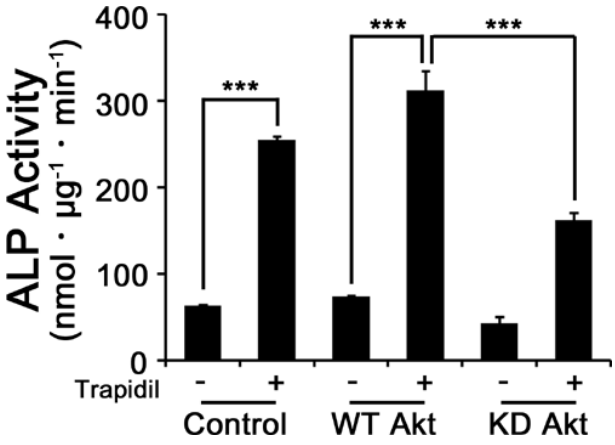
ALP Activity
(nmol · μg-1 · min-1)
400
300
200
100
0
***
***
***
Trapidil
-
+
-
+
-
+
Control
WT Akt
KD Akt

C

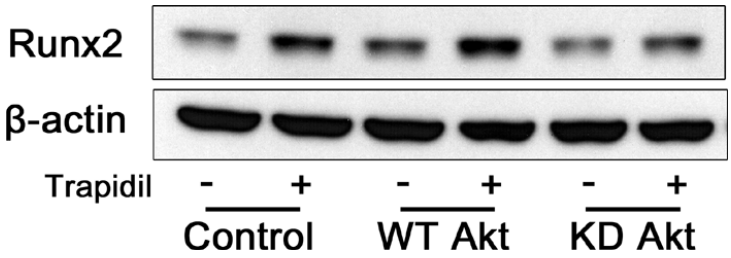
Runx2
β-actin
Trapidil
-
+
-
+
-
+
Control
WT Akt
KD Akt

**Figure 24. Akt is involved in trapidil-induced osteogenesis**

(A-C) Mouse calvarial osteoblast precursors were electroporated with vectors which are pMSCV empty vector; control vector, pMSCV-Akt-WT, and pMSCV-Akt-KD and then cultured for 24 hours. (A) The cells were cultured in osteogenic medium with or without trapidil (400 μM). ALP staining (A, *top panel*) and ALP activity assay in cell lysates (B) were assayed on day 3. Alizarin red S staining was performed on day 14 (A, *bottom panel*) (C) Whole-cell lysates were subjected to immunoblotting with the indicated antibodies on day 2. The results shown are representative of three independent experiments (n=3), and the values are expressed as mean ± SD. ***P < 0.001 by unpaired Student's *t* test.

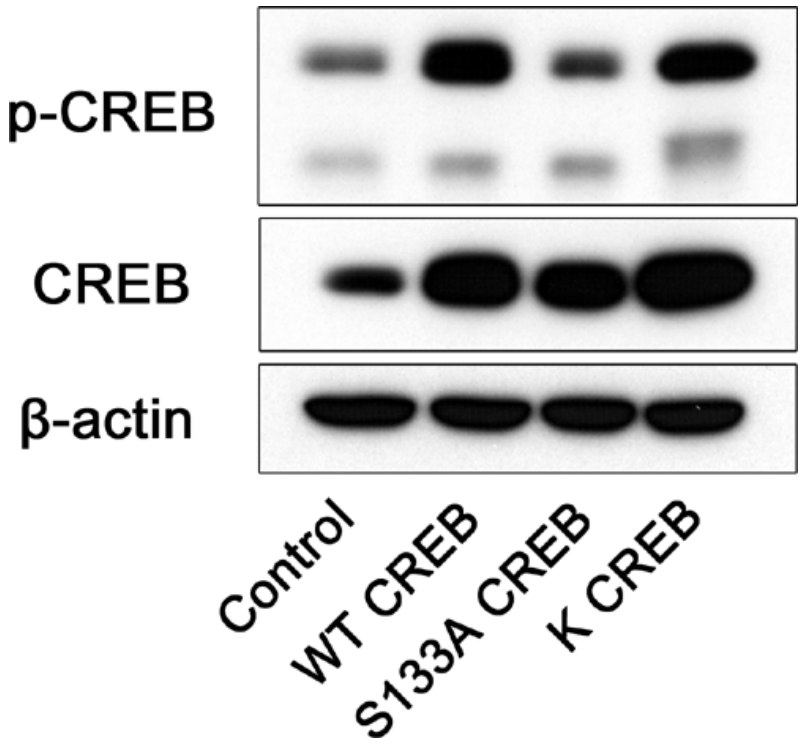


**Figure 25. Overexpression of CREB constructs in calvarial osteoblasts**

Mouse calvarial osteoblast precursors were infected with retro virus containing vectors which are pMX-puro empty vector; control vector, pMX-puro-WT CREB, pMX-puro-S133A CREB, and pMX-puro-K CREB. The cells were cultured for 24 hours after electroporation and then whole-cell lysates were subjected to immunoblotting with the indicated antibodies. The results shown are representative of three independent experiments

A

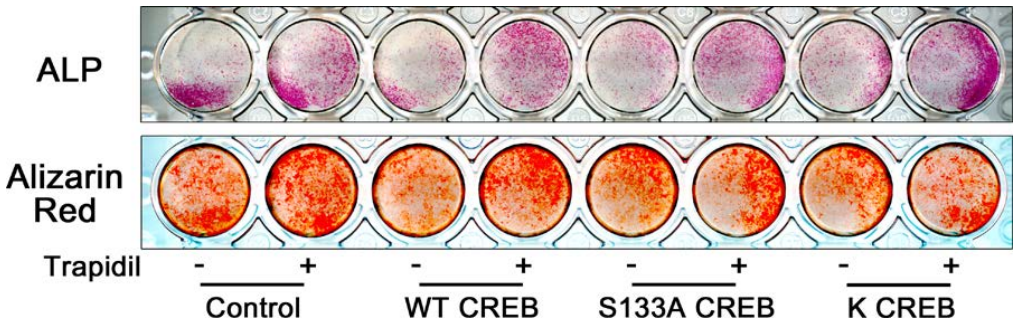
ALP
Alizarin Red
Trapidil
-
+
Control
WT CREB
S133A CREB
K CREB

B

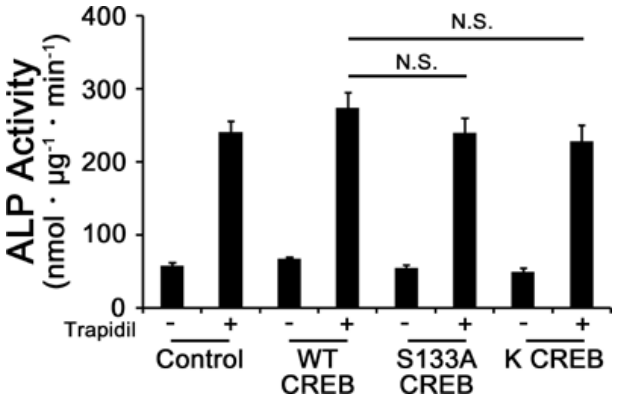
ALP Activity
(nmol · μg⁻¹ · min⁻¹)
400
300
200
100
0
N.S.
N.S.
Trapidil
Control
WT CREB
S133A CREB
K CREB

C

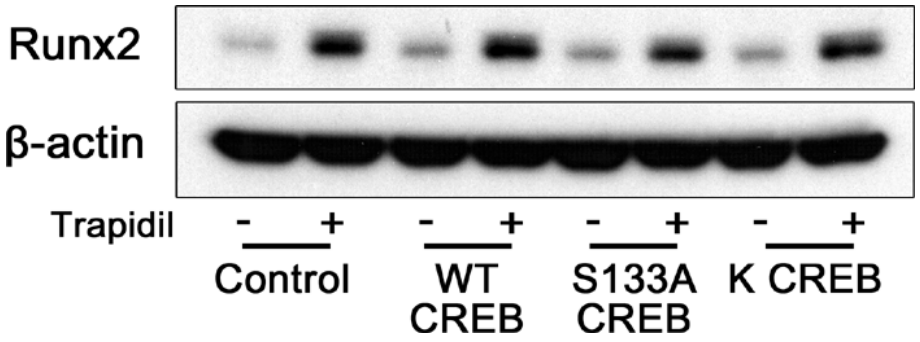
Runx2
β-actin
Trapidil
Control
WT CREB
S133A CREB
K CREB

**Figure 26. CREB is not involved in trapidil-induced osteogenesis**

(A-C) Mouse calvarial osteoblast precursors were infected with retro virus containing vectors which are pMX-puro empty vector; control vector, pMX-puro-WT CREB, pMX-puro-S133A CREB, and pMX-puro-K CREB and then cultured for 24 hours. (A) The cells were cultured in osteogenic medium with or without trapidil (400 μM). ALP staining (A, *top panel*) and ALP activity assay in cell lysates (B) were assayed on day 3. Alizarin red S staining was performed on day 14 (A, *bottom panel*) (C) Whole-cell lysates were subjected to immunoblotting with the indicated antibodies on day 2. The results shown are representative of three independent experiments (n=3), and the values are expressed as mean ± SD. N.S., not significant

## Trapidil inhibits PDGFRα

Next, the status of PDGFRs exposed to trapidil was investigated. PDGFs have different affinities to each PDGFR. Specifically, PDGF-BB binds to and activates all PDGFRs and has a strong affinity to PDGFRβ, whereas PDGF-AA binds to and activates only PDGFRα (*16*). As expected, trapidil inhibited PDGF-AA-induced phosphorylation of PDGFRs and its downstream molecule, ERK (Figure 27A). However, trapidil did not inhibit PDGF-BB-induced phosphorylation of PDGFRs and ERK (Figure 27B). In addition, cell proliferation induced by PDGF-AA was completely blocked by a high concentration of trapidil (1 mM, Figure 28A). However, PDGF-BB-induced cell proliferation was not completely blocked by a high concentration of trapidil (1 mM), which slightly inhibited it (Figure 28B). Taken together, these data indicate that trapidil inhibited PDGFRα more effectively than it did PDGFRβ, at least in the osteoblasts. Moreover, 400 μM. trapidil, the highest concentration used for osteogenesis in this study, inhibited only PDGFRα and not PDGFRβ, suggesting that trapidil activated BMP signaling by inhibiting PDGFRα.

A

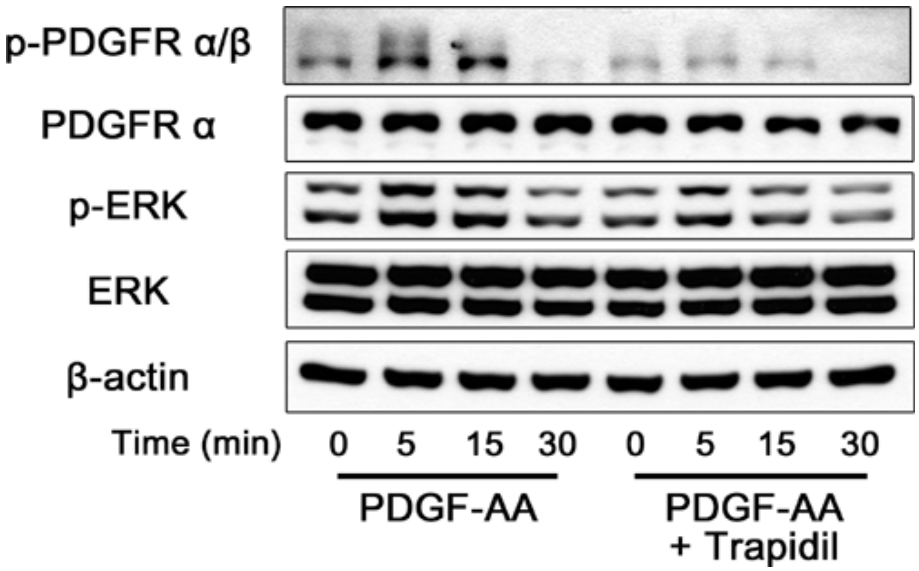
p-PDGFR α/β
PDGFR α
p-ERK
ERK
β-actin
Time (min) 0 5 15 30 0 5 15 30
PDGF-AA
PDGF-AA
+ Trapidil

B

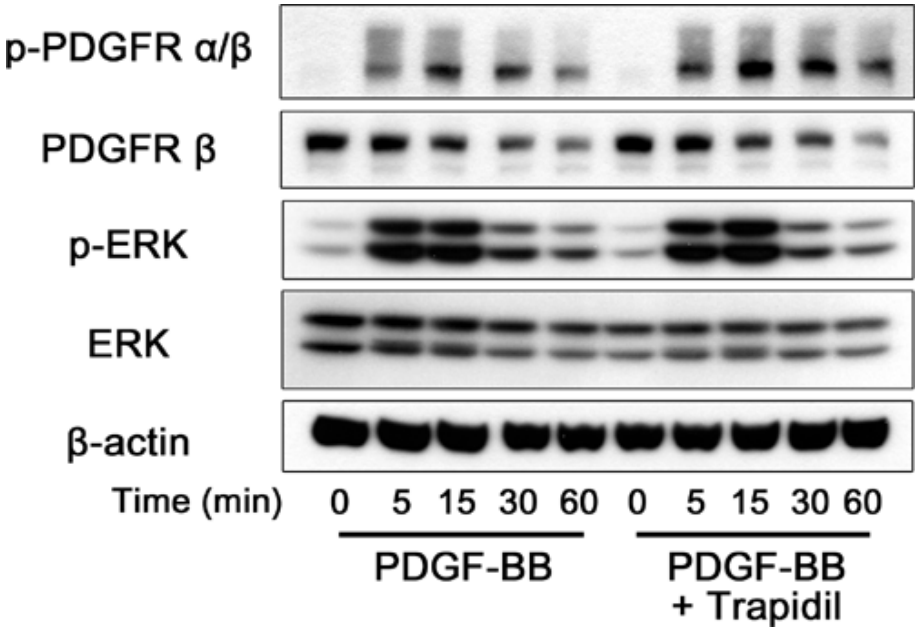
p-PDGFR α/β
PDGFR β
p-ERK
ERK
β-actin
Time (min) 0 5 15 30 60 0 5 15 30 60
PDGF-BB
PDGF-BB
+ Trapidil

**Figure 27. Trapidil inhibits PDGF-AA-induced activation of PDGFRs, and does not inhibits PDGF-BB-induced activation of PDGFRs**

(A, B) Mouse calvarial osteoblast precursors were pre treated with DMSO or trapidil (400 μM) for 4 hours. (A) The cells were then treated with PDGF-AA (20 ng/ml) for the indicated times and whole-cell lysates were subjected to immunoblotting with the indicated antibodies. (B) The cells were then treated with PDGF-BB (20 ng/ml) for the indicated times and whole-cell lysates were subjected to immunoblotting with the indicated antibodies.

A

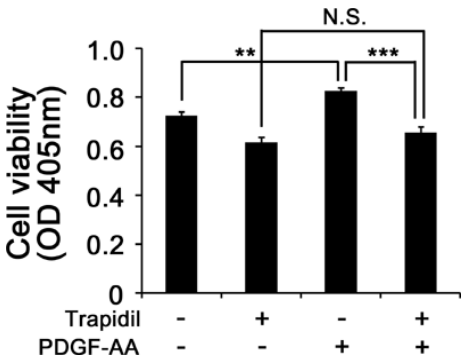


B

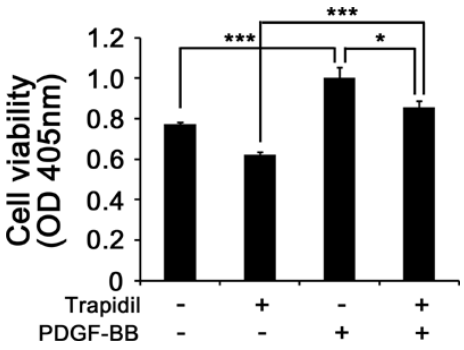


**Figure 28. Trapidil completely blocked PDGF-AA-induced cell proliferation**

(A) Mouse calvarial osteoblast precursors were cultured in osteogenic medium with DMSO or trapidil (1 mM) in the presence or absence of PDGF-AA (20ng/ml) for 24 hours and then cell viabilities were measured. (B) Mouse calvarial osteoblast precursors were cultured in osteogenic medium with DMSO or trapidil (1 mM) in the presence or absence of PDGF-BB (20ng/ml) for 24 hours and then cell viabilities were measured. The results shown are representative of three independent experiments (n=3), and the values are expressed as mean ± SD. *P < 0.05; **P < 0.01; ***P < 0.001 *vs.* untreated control by unpaired Student's *t* test.

## Discussion

Trapidil has been reported to be effective against human coronary artery disease (*37*). In addition, several studies have shown that trapidil is effective in several animal disease models including ischemia-reperfusion injury, oxidative organ damage in burn injury, gentamicin nephrotoxicity, and hyperparathyroidism (*32, 39, 55, 56*). In this study, the *in vitro* and *in vivo* pro-osteogenic effects of trapidil were demonstrated for the first time.

Accumulating evidence from genetic and pharmacologic studies has revealed that PDGFR signaling inhibits osteogenic differentiation (*26*). Both depletion of PDGFRβ and inhibition of PDGFRs by imatinib or AG-1295 have been shown to promote osteoblast differentiation (*25, 27, 28*). Consistent with these reports, trapidil, a PDGFR antagonist also promoted osteogenesis without affecting cell viability even at the highest concentrations used for osteogenesis in our study. Trapidil treatment increased the early signals including phosphorylation of Smad1/5/8 and MAPKs, Runx2 upregulation, and ALP activity, similar to the BMPR-activated downstream cascades, thereby promoting osteogenesis (Figures 6–12).

Several BMPs, including BMP-2, -4, -5, -6, and -7, are produced during

osteoblast differentiation (*57-60*). Notably, it has been reported that autocrine BMP signaling is involved in osteoblast differentiation not only during the early phase of differentiation but also during matrix maturation and mineralization (*61*). In the present study, trapidil induced osteogenesis even in the absence of exogenously administered BMPs (Figures 6 and 7). The effects of ALK3 depletion and LDN193189 treatment showed that BMPR activity is required for the trapidil-induced osteogenesis (Figures 14 and 18). Thus, whether trapidil influences the autocrine BMP signaling-induced BMPR activation was investigated. Although trapidil did not affect BMP expression, the trapidil-induced Smad1/5/9 phosphorylation was abolished by removing BMP-expressing osteoblasts from the culture supernatant (Figure 20). Consistent with this result, noggin treatment blocked the trapidil-induced Smad1/5/9 phosphorylation, Runx2 expression, ALP activity, and calcium deposition, indicating that trapidil required autocrine BMP signaling for BMPR activation and osteogenesis (Figure 21). Furthermore, the effects of exogenously administered BMP2-induced Smad1/5/9 phosphorylation, Runx2 expression, and calcium deposition were amplified in the presence of trapidil compared with BMP2 treatment alone (Figure 22), which suggests that trapidil likely increases BMP signaling. In addition, blocking PDGF signaling with imatinib, PDGFR inhibitor IV, and PDGFR inhibitor V (other known PDGFR inhibitors)

also increased the mineralization and phosphorylation of Smad1/5/9, suggesting that inhibiting PDGFR may activate BMP signaling (Figures 15 and 16). Moreover, under minimized autocrine BMP conditions, trapidil did not activate Smad1/5/9, suggesting that trapidil could not activate BMPRs directly (Figure 20). Taken together, these data indicate that trapidil may increase the susceptibility of BMPR, perhaps mediated by ALK3 through the inhibition of PDGFRs, leading to enhanced osteogenesis (Figure 28). However, it is uncertain whether inhibition of PDGFR affects the binding capacity of BMPR to BMP or the activity of BMPR to initiate downstream pathway cascades. Thus, the detailed mechanisms by which inhibition of PDGFR signaling increases BMP signaling remain to be elucidated.

The osteogenic differentiation process is complicated and involves various signaling pathways and mediators. The phosphoinositide 3-kinase (PI3K)/Akt signaling axis is one of the osteogenic mediators. Akt1 knockout mice have shown reduced bone mineral density (*62*) and mice with osteoblast-specific depletion of phosphatase and tensin homolog (PTEN), a negative regulator of PI3K/Akt signaling, show increased bone formation due to the elevated Akt-mediated cell survival (*63*). In addition, Akt promotes BMP-induced osteogenic differentiation *in vitro,* and PI3K/Akt signaling is required for BMP-induced Osx transcriptional activity (*52, 53, 64*). In this study, Akt

was also activated by trapidil (Figure 11) and transduction of dominant negative Akt inhibited trapidil-induced osteogenesis (Figure 24). In line with this, trapidil-promoted osteogenic differentiation was also inhibited by LY294002, a PI3K inhibitor (data not shown). These data demonstrate that trapidil-activated Akt was also involved in the trapidil-induced osteogenic differentiation, at least in part (Figure 28).

Cell proliferation and differentiation usually show inverse relationship. In our study, trapidil at concentrations up to 400 μM increased osteogenic differentiation without affecting cell viability (Figure 6–9). However, a high concentration of trapidil (2 mM) inhibited mineralization and proliferation of osteoblasts despite the increased ALP activity (Figure 10). Studies have shown that cell number affects osteoblast differentiation, and cell proliferation in the early phase of osteoblast differentiation is important to osteogenic differentiation (*65, 66*). In addition, Chen et al. (*67*) have shown that high concentration of PDGF-BB inhibited osteoblastic differentiation and weakened the bone strength and low concentration of PDGF-BB promoted osteoblastic differentiation and raise bone strength both in-vitro and in-vivo (*67*). Taken together, these results indicate that strong regulation of PDGF signaling may cause an imbalance between proliferation and differentiation of osteoblasts or osteoblast precursor cells, leading to bone weakening. Therefore, PDGFs

signaling should be delicately regulated to some degree for therapeutic applications.

Imatinib is a tyrosine kinase inhibitor of ABL proto-oncogene 1, non-receptor tyrosine kinase (c-abl) and KIT proto-oncogene receptor tyrosine kinase (c-kit) that has been shown to promote osteogenesis *in vitro* by inhibiting PDGF signaling. However, imatinib does not increase bone volume *in vivo* but, rather, it reduces trabecular bone volume, osteoblast surface, and serum osteocalcin (*68*). Several studies have shown that mice lacking c-abl or c-kit show decreased bone mass (*69, 70*). The unexpected effects of imatinib on bone *in vivo* might be due to an inhibition of the important kinases required for bone formation. Unlike the findings for imatinib, in the present study, administration of trapidil stimulated bone regeneration in our animal model (Figure 1).

Currently, most osteoporosis medications are anti-resorptive drugs such as selective estrogen receptor modulators (SERMs), bisphosphonate, and denosumab (an anti-receptor activator of nuclear factor κ-B ligand [RANKL] antibody) that inhibit osteoclast-mediated bone resorption (*71*). However, inhibition of bone resorption alone may not be sufficient for the treatment of osteoporosis. Combined anti-resorptive and bone anabolic therapy may be more effective for osteoporosis therapy. Our previous (*40*) and present study have revealed that trapidil exerts both an anti-osteoclastogenic effect and a pro-

osteogenic effect. Thus, trapidil may be promising for osteoporosis therapy based on its dual actions.

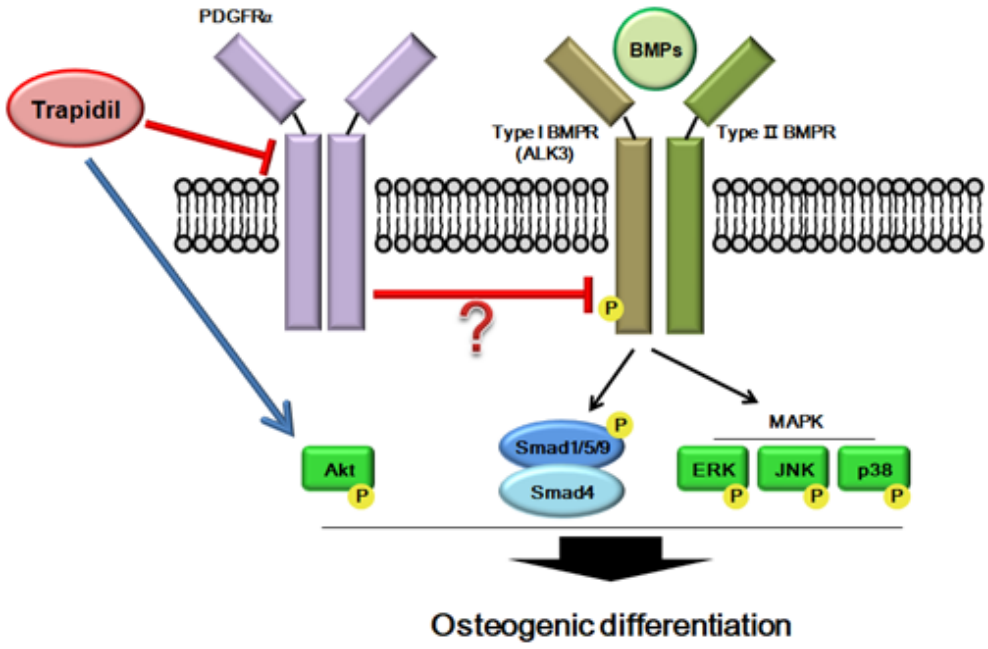


**Figure 28. Osteogenic mechanisms of trapidil**

PDGFRs may inhibit BMPRs through unknown mechanism. Among those, PDGFRα perhaps inhibits one of BMP type I receptor, ALK3. Trapidil inhibits PDGFRα in osteoblasts leading to increase activity of ALK3. ALK3 with elevated activity activates its downstream such as Smad1/5/9, ERK, JNK, and p38 under stimuli of BMPs. Trapidil also activates Akt through unknown mechanism. These activated Smad1/5/9, ERK, JNK, p38, and Akt increases Runx2 expression and elevates genes for osteogenic differentiation. Through mechanisms described above, trapidil promote bone healing and osteogenic differentiation both *in vivo* and *in vitro*.

# V. Reference


1. L. G. Raisz, Pathogenesis of osteoporosis: concepts, conflicts, and prospects. *The Journal of clinical investigation* 115, 3318-3325 (2005).
2. M. Kawai, U. I. Modder, S. Khosla, C. J. Rosen, Emerging therapeutic opportunities for skeletal restoration. *Nature reviews. Drug discovery* 10, 141-156 (2011).
3. B. L. Riggs, The mechanisms of estrogen regulation of bone resorption. *The Journal of clinical investigation* 106, 1203-1204 (2000).
4. I. R. Reid, Short-term and long-term effects of osteoporosis therapies. *Nature reviews. Endocrinology* 11, 418-428 (2015).
5. J. L. Vahle *et al.*, Bone neoplasms in F344 rats given teriparatide [rhPTH(1-34)] are dependent on duration of treatment and dose. *Toxicologic pathology* 32, 426-438 (2004).
6. E. Canalis, Growth factor control of bone mass. *Journal of cellular biochemistry* 108, 769-777 (2009).
7. M. R. Urist, B. S. Strates, The classic: Bone morphogenetic protein. *Clinical orthopaedics and related research* 467, 3051-3062 (2009).
8. K. Miyazono, S. Maeda, T. Imamura, BMP receptor signaling: transcriptional targets, regulation of signals, and signaling cross-talk. *Cytokine & growth factor reviews* 16, 251-263 (2005).
9. O. Korchynskyi, P. ten Dijke, Identification and functional

characterization of distinct critically important bone morphogenetic protein-specific response elements in the Id1 promoter. *The Journal of biological chemistry* 277, 4883-4891 (2002).

10. A. Moustakas, C. H. Heldin, The regulation of TGFbeta signal transduction. *Development (Cambridge, England)* 136, 3699-3714 (2009).
11. V. S. Salazar, L. W. Gamer, V. Rosen, BMP signalling in skeletal development, disease and repair. *Nature reviews. Endocrinology* 12, 203-221 (2016).
12. M. S. Rahman, N. Akhtar, H. M. Jamil, R. S. Banik, S. M. Asaduzzaman, TGF-beta/BMP signaling and other molecular events: regulation of osteoblastogenesis and bone formation. *Bone research* 3, 15005 (2015).
13. W. Huang, S. Yang, J. Shao, Y. P. Li, Signaling and transcriptional regulation in osteoblast commitment and differentiation. *Frontiers in bioscience : a journal and virtual library* 12, 3068-3092 (2007).
14. K. S. Lee, S. H. Hong, S. C. Bae, Both the Smad and p38 MAPK pathways play a crucial role in Runx2 expression following induction by transforming growth factor-beta and bone morphogenetic protein. *Oncogene* 21, 7156-7163 (2002).
15. P. Ducy, Cbfa1: a molecular switch in osteoblast biology. *Developmental dynamics : an official publication of the American Association of Anatomists* 219, 461-471 (2000).
16. R. V. Hoch, P. Soriano, Roles of PDGF in animal development.

*Development (Cambridge, England)* 130, 4769-4784 (2003).
17. C. H. Heldin, B. Westermark, Mechanism of action and in vivo role of platelet-derived growth factor. *Physiological reviews* 79, 1283-1316 (1999).
18. G. A. Currie, Platelet-derived growth-factor requirements for in vitro proliferation of normal and malignant mesenchymal cells. *British journal of cancer* 43, 335-343 (1981).
19. M. Hosang *et al.*, Both homodimeric isoforms of PDGF (AA and BB) have mitogenic and chemotactic activity and stimulate phosphoinositol turnover. *Journal of cellular physiology* 140, 558-564 (1989).
20. H. Fujii, R. Kitazawa, S. Maeda, K. Mizuno, S. Kitazawa, Expression of platelet-derived growth factor proteins and their receptor alpha and beta mRNAs during fracture healing in the normal mouse. *Histochemistry and cell biology* 112, 131-138 (1999).
21. Y. Ozaki *et al.*, Comprehensive analysis of chemotactic factors for bone marrow mesenchymal stem cells. *Stem cells and development* 16, 119-129 (2007).
22. L. G. Chase, U. Lakshmipathy, L. A. Solchaga, M. S. Rao, M. C. Vemuri, A novel serum-free medium for the expansion of human mesenchymal stem cells. *Stem cell research & therapy* 1, 8 (2010).
23. M. A. Sanchez-Fernandez, A. Gallois, T. Riedl, P. Jurdic, B. Hoflack, Osteoclasts control osteoblast chemotaxis via PDGF-BB/PDGF receptor beta signaling. *PloS one* 3, e3537 (2008).

24. Y. Wu, Y. Zhang, Q. Yin, H. Xia, J. Wang, Plateletderived growth factor promotes osteoblast proliferation by activating Gproteincoupled receptor kinase interactor1. *Molecular medicine reports* 10, 1349-1354 (2014).
25. A. Tokunaga *et al.*, PDGF receptor beta is a potent regulator of mesenchymal stromal cell function. *Journal of bone and mineral research : the official journal of the American Society for Bone and Mineral Research* 23, 1519-1528 (2008).
26. K. Kubota, C. Sakikawa, M. Katsumata, T. Nakamura, K. Wakabayashi, PDGF BB purified from osteoclasts acts as osteoblastogenesis inhibitory factor (OBIF). *Journal of biomolecular techniques : JBT* 13, 62-71 (2002).
27. Y. Y. Zhang *et al.*, Platelet-derived growth factor receptor kinase inhibitor AG-1295 promotes osteoblast differentiation in MC3T3-E1 cells via the Erk pathway. *Bioscience trends* 6, 130-135 (2012).
28. S. O'Sullivan *et al.*, Imatinib promotes osteoblast differentiation by inhibiting PDGFR signaling and inhibits osteoclastogenesis by both direct and stromal cell-dependent mechanisms. *Journal of bone and mineral research : the official journal of the American Society for Bone and Mineral Research* 22, 1679-1689 (2007).
29. J. Deguchi, J. Abe, M. Makuuchi, Y. Takuwa, Inhibitory effects of trapidil on PDGF signaling in balloon-injured rat carotid artery. *Life sciences* 65, 2791-2799 (1999).
30. M. Hoshiya, M. Awazu, Trapidil inhibits platelet-derived growth

factor-stimulated mitogen-activated protein kinase cascade. *Hypertension (Dallas, Tex. : 1979)* 31, 665-671 (1998).

31. L. Gesualdo, S. Di Paolo, E. Ranieri, F. P. Schena, Trapidil inhibits human mesangial cell proliferation: effect on PDGF beta-receptor binding and expression. *Kidney international* 46, 1002-1009 (1994).
32. K. Buyukafsar *et al.*, Effect of trapidil, an antiplatelet and vasodilator agent on gentamicin-induced nephrotoxicity in rats. *Pharmacological research* 44, 321-328 (2001).
33. A. V. Mazurov, M. Menshikov, V. L. Leytin, V. A. Tkachuk, V. S. Repin, Decrease of platelet aggregation and spreading via inhibition of the cAMP phosphodiesterase by trapidil. *FEBS letters* 172, 167-171 (1984).
34. H. Ohnishi *et al.*, Effects of trapidil on thromboxane A2-induced aggregation of platelets, ischemic changes in heart and biosynthesis of thromboxane A2. *Prostaglandins and medicine* 6, 269-281 (1981).
35. L. Zhou *et al.*, Inhibition of the CD40 pathway of monocyte activation by triazolopyrimidine. *Clinical immunology (Orlando, Fla.)* 93, 232-238 (1999).
36. O. J. Sichelschmidt, C. Hahnefeld, T. Hohlfeld, F. W. Herberg, K. Schror, Trapidil protects ischemic hearts from reperfusion injury by stimulating PKAII activity. *Cardiovascular research* 58, 602-610 (2003).
37. S. Okamoto, M. Inden, M. Setsuda, T. Konishi, T. Nakano, Effects of trapidil (triazolopyrimidine), a platelet-derived growth factor

antagonist, in preventing restenosis after percutaneous transluminal coronary angioplasty. *American heart journal* 123, 1439-1444 (1992).

38. S. Lotinun, J. D. Sibonga, R. T. Turner, Triazolopyrimidine (trapidil), a platelet-derived growth factor antagonist, inhibits parathyroid bone disease in an animal model for chronic hyperparathyroidism. *Endocrinology* 144, 2000-2007 (2003).
39. R. T. Turner, U. T. Iwaniec, K. Marley, J. D. Sibonga, The role of mast cells in parathyroid bone disease. *Journal of bone and mineral research : the official journal of the American Society for Bone and Mineral Research* 25, 1637-1649 (2010).
40. S. D. Kim *et al.*, Trapidil, a platelet-derived growth factor antagonist, inhibits osteoclastogenesis by down-regulating NFATc1 and suppresses bone loss in mice. *Biochemical pharmacology* 86, 782-790 (2013).
41. C. Kilkenny, W. Browne, I. C. Cuthill, M. Emerson, D. G. Altman, Animal research: reporting in vivo experiments: the ARRIVE guidelines. *British journal of pharmacology* 160, 1577-1579 (2010).
42. J. C. McGrath, E. Lilley, Implementing guidelines on reporting research using animals (ARRIVE etc.): new requirements for publication in BJP. *British journal of pharmacology* 172, 3189-3193 (2015).
43. T. M. Sweeney, L. A. Opperman, J. A. Persing, R. C. Ogle, Repair of critical size rat calvarial defects using extracellular matrix protein gels. *Journal of neurosurgery* 83, 710-715 (1995).

44. P. P. Spicer *et al.*, Evaluation of bone regeneration using the rat critical size calvarial defect. *Nature protocols* 7, 1918-1929 (2012).
45. H. N. Kim *et al.*, Histone deacetylase inhibitor MS-275 stimulates bone formation in part by enhancing Dhx36-mediated TNAP transcription. *Journal of bone and mineral research : the official journal of the American Society for Bone and Mineral Research* 26, 2161-2173 (2011).
46. M. Soleimani, S. Nadri, A protocol for isolation and culture of mesenchymal stem cells from mouse bone marrow. *Nature protocols* 4, 102-106 (2009).
47. J. Son, J. H. Lee, H. N. Kim, H. Ha, Z. H. Lee, cAMP-response-element-binding protein positively regulates breast cancer metastasis and subsequent bone destruction. *Biochemical and biophysical research communications* 398, 309-314 (2010).
48. M. J. Curtis *et al.*, Experimental design and analysis and their reporting: new guidance for publication in BJP. *British journal of pharmacology* 172, 3461-3471 (2015).
49. T. F. Li *et al.*, Parathyroid hormone-related peptide (PTHrP) inhibits Runx2 expression through the PKA signaling pathway. *Experimental cell research* 299, 128-136 (2004).
50. D. C. Yang *et al.*, cAMP/PKA regulates osteogenesis, adipogenesis and ratio of RANKL/OPG mRNA expression in mesenchymal stem cells by suppressing leptin. *PloS one* 3, e1540 (2008).
51. A. M. Osyczka, P. S. Leboy, Bone morphogenetic protein

regulation of early osteoblast genes in human marrow stromal cells is mediated by extracellular signal-regulated kinase and phosphatidylinositol 3-kinase signaling. *Endocrinology* 146, 3428-3437 (2005).

52. A. Mukherjee, P. Rotwein, Akt promotes BMP2-mediated osteoblast differentiation and bone development. *Journal of cell science* 122, 716-726 (2009).

53. A. Mukherjee, E. M. Wilson, P. Rotwein, Selective signaling by Akt2 promotes bone morphogenetic protein 2-mediated osteoblast differentiation. *Molecular and cellular biology* 30, 1018-1027 (2010).

54. H. Zhang *et al.*, Activation of PKA/CREB Signaling is Involved in BMP9-Induced Osteogenic Differentiation of Mesenchymal Stem Cells. *Cellular physiology and biochemistry : international journal of experimental cellular physiology, biochemistry, and pharmacology* 37, 548-562 (2015).

55. D. Avlan *et al.*, Protective effect of trapidil against oxidative organ damage in burn injury. *Burns : journal of the International Society for Burn Injuries* 31, 859-865 (2005).

56. S. Somuncu *et al.*, Protective effects of trapidil in lung after abdominal aorta induced ischemia-reperfusion injury: an experimental study. *Pediatric surgery international* 21, 983-988 (2005).

57. Y. Okubo, K. Bessho, K. Fujimura, T. Iizuka, S. Miyatake, Expression of bone morphogenetic protein-2 via adenoviral vector in C2C12 myoblasts induces differentiation into the

osteoblast lineage. *Biochemical and biophysical research communications* 262, 739-743 (1999).

58. A. Yamaguchi *et al.*, Effects of BMP-2, BMP-4, and BMP-6 on osteoblastic differentiation of bone marrow-derived stromal cell lines, ST2 and MC3T3-G2/PA6. *Biochemical and biophysical research communications* 220, 366-371 (1996).
59. F. J. Hughes, J. Collyer, M. Stanfield, S. A. Goodman, The effects of bone morphogenetic protein-2, -4, and -6 on differentiation of rat osteoblast cells in vitro. *Endocrinology* 136, 2671-2677 (1995).
60. I. Asahina, T. K. Sampath, I. Nishimura, P. V. Hauschka, Human osteogenic protein-1 induces both chondroblastic and osteoblastic differentiation of osteoprogenitor cells derived from newborn rat calvaria. *The Journal of cell biology* 123, 921-933 (1993).
61. G. van der Horst *et al.*, Differentiation of murine preosteoblastic KS483 cells depends on autocrine bone morphogenetic protein signaling during all phases of osteoblast formation. *Bone* 31, 661-669 (2002).
62. N. Kawamura *et al.*, Akt1 in osteoblasts and osteoclasts controls bone remodeling. *PloS one* 2, e1058 (2007).
63. A. R. Guntur, M. I. Reinhold, J. Cuellar, Jr., M. C. Naski, Conditional ablation of Pten in osteoprogenitors stimulates FGF signaling. *Development (Cambridge, England)* 138, 1433-1444 (2011).
64. C. C. Mandal, H. Drissi, G. G. Choudhury, N. Ghosh-Choudhury,

Integration of phosphatidylinositol 3-kinase, Akt kinase, and Smad signaling pathway in BMP-2-induced osterix expression. *Calcified tissue international* 87, 533-540 (2010).

65. X. Chen *et al.*, Developing osteoblasts as an endpoint for the mouse embryonic stem cell test. *Reproductive toxicology (Elmsford, N.Y.)* 53, 131-140 (2015).
66. L. Malaval, F. Liu, P. Roche, J. E. Aubin, Kinetics of osteoprogenitor proliferation and osteoblast differentiation in vitro. *Journal of cellular biochemistry* 74, 616-627 (1999).
67. W. Chen *et al.*, PDGFB-based stem cell gene therapy increases bone strength in the mouse. *Proceedings of the National Academy of Sciences of the United States of America* 112, E3893-3900 (2015).
68. S. O'Sullivan *et al.*, Imatinib mesylate does not increase bone volume in vivo. *Calcified tissue international* 88, 16-22 (2011).
69. S. Lotinun, N. Krishnamra, Disruption of c-Kit Signaling in Kit(W-sh/W-sh) Growing Mice Increases Bone Turnover. *Scientific reports* 6, 31515 (2016).
70. B. Li *et al.*, Mice deficient in Abl are osteoporotic and have defects in osteoblast maturation. *Nature genetics* 24, 304-308 (2000).
71. J. S. Chen, P. N. Sambrook, Antiresorptive therapies for osteoporosis: a clinical overview. *Nature reviews. Endocrinology* 8, 81-91 (2011).

# BMP2 신호전달 활성화를 통한

# 트라피딜의 골 형성 촉진

서울대학교 치의학대학원 세포및발생생물학 교실

(지도교수 **이 장 희**)

**김 봉 준**

골은 파골세포와 골모세포에 의해 정교하게 균형을 이루며 끊임없이 골개조(remodeling)가 일어나는 조직으로, 과도한 골흡수 촉진으로 인한 골개조의 불균형은 골다공증과 같은 골소실성 질병을 유발한다. 이러한 골다공증을 치료하기 위하여 증가된 파골세포의 활성을 억제하는 약물들이 사용되고 있지만, 이미 소실된 골을 복원하지 못하기 때문에 골형성을 촉진하는 약물 개발이 요구되고 있다.

기존 연구에 의하면 성장인자 중 하나인 혈소판 유래 성장인자 (Platelet-derived growth factor, PDGF) 신호전달 경로를 억제하면 시험관내실험에서 골모세포 분화를 촉진한다고 알려져 있다. 하지만 이

러한 PDGF 신호전달경로 억제를 통한 골형성 촉진효과는 아직 동물 모델을 이용한 생체실험에서 입증되지 않았고, PDGF 수용체 억제제가 어떠한 기전을 통해 골형성을 촉진하는지에 대해서도 아직 연구되지 않았다.

본 연구는 시험관내 실험 및 생체실험에서 PDGF 수용체의 길항자(antagonist)인 트라피딜(trapidil)의 골형성 촉진 효과를 연구하고 그 기전을 규명하고자 하였다. 생체실험에서 트라피딜의 골형성 촉진 효과를 검증하기 위해 흰쥐 두개골 결손 모델을 사용하였으며, 마이크로 컴퓨터 단층촬영 및 조직검사를 통해 분석한 결과 트라피딜이 골형성을 촉진하는 것을 확인하였다. 또한 트라피딜의 작용기전을 연구하기 위해 마우스 두개골 골모세포 전구체를 사용하여 시험관내실험으로 연구하였다. 그 결과 트라피딜이 뼈형성단백질(bone morphogenetic protein, BMP) 신호전달경로를 활성화하여 골형성을 촉진

한다는 것을 규명하였다. 또한 BMP 수용체 발현억제 실험을 통해 트라피딜은 BMP 수용체중 액티빈 수용체유사유전체 3(activin receptor-like kinase3, ALK3)를 활성화하여 골형성을 촉진한다는 것을 확인하였다. 추가적인 실험을 통해 트라피딜은 직접적으로 ALK3를 활성화 하는 것이 아니라, PDGF 수용체 억제를 통해 ALK3를 활성화 하는 것을 확인하였다.

본 연구결과를 종합하면, 트라피딜은 PDGF 수용체를 억제하여 ALK3를 활성화하고, 나아가 BMP 수용체 신호전달경로를 활성화하여 골형성을 촉진함을 규명하였다.

---

주요어 : 트라피딜, 골모세포, PDGF, BMP, 골형성

학 번 : 2013-23553